Exploring the Nuclear Translocation of TPL2 and Its Interaction with MEK1

Xiaofeng Shi

School of Molecular Biosciences

College of Medical, Veterinary and Life Sciences (MVLS)

University of Glasgow

Abstract

The mitogen-activated protein kinase (MAPK) signalling pathway is a conserved pathway involved in cell proliferation, survival, and therapeutic resistance. TPL2 (also known as MAP3K8) functions as a serine/threonine kinase upstream of the MAPK cascade. By activating MEK1/2 and ERK1/2, it triggers the production of pro-inflammatory cytokines such as TNF-α and IL-6, thereby regulating inflammatory immune responses and transmitting cellular signals. Additionally, TPL2 modulates cell proliferation and survival. Collins et al, (2019) previously demonstrated that TPL2 shuttles between the nucleus and cytoplasm via a CRM1-dependent nuclear export mechanism mediated by its NES motif, confirming its transport into the nucleus followed by rapid degradation by the proteasome. However, the regulatory mechanisms governing its nuclear transport and the significance of its nuclear-cytoplasmic shuttling as an upstream scaffold protein in signal transduction remain unclear.

This study revealed TPL2's role in subcellular signalling organization by analysing the structural components guiding its nuclear entry and its ability to interact with MEK1. This study constructed a TPL2 kinase-inactive mutant ($TPL2^{D270A}$) and MEK1 mutants with nuclear import defects (T218A/T222A/T226A) through site-directed mutagenesis to investigate their intracellular dynamics and evaluate their colocalization patterns with two TPL2 structural mutants: a C-terminal truncation mutant (TPL2ΔC, lacking residues 397-467 that include a putative degradation motif), and a NES deletion mutant (TPL2ΔNES, lacking the nuclear export signal), co-expressed in HEK293 cells. The behavioural characteristics of the mutant proteins were assessed using subcellular fractionation combined with immunoprecipitation, Western blotting, and confocal imaging techniques.

This study shows that the deletion of the C-terminal region can stabilize TPL2 and increase ERK phosphorylation. The kinase activity of TPL2 contributes to the stabilization of MEK1, and removal of the inhibitory C-terminal domain further

enhances this effect. These findings are consistent with previous reports suggesting that the C-terminal region functions as a negative regulatory domain (Gantke et al.,2011). Additionally, this study observed that the activation and stable expression of MEK1 the kinase activity of TPL2. More intriguingly, TPL2 promotes nuclear accumulation of MEK1 mutants with nuclear import defects. These results indicate that TPL2 may assist MEK1 nuclear import even when MEK1's own import signal is defective, suggesting that TPL2 contributes to MEK1 subcellular localization through a non-catalytic, potentially scaffold-like mechanism rather than solely through kinase-dependent signalling, as observed in the co-expression experiments with MEK1 mutants and TPL2 mutants.

In summary, this study reveals that TPL2 contributes to the subcellular localization and stabilization of MEK1 through both its kinase activity and structural domains. Specifically, co-expression experiments using MEK1 mutants with impaired nuclear import signals showed that TPL2 facilitates MEK1 nuclear accumulation, even in the absence of canonical import motifs. This suggests that TPL2 may function as a scaffold-like carrier in addition to its catalytic role. These findings highlight a previously unrecognized bidirectional interaction between MEK1 and TPL2, where TPL2 regulates MEK1 localization, and MEK1 mutants, in turn, reveal regulatory features of TPL2 localization. This expands our understanding of MAPK pathway regulation through subcellular localization dynamics and suggests new potential targets for therapeutic intervention.

However, several limitations should be acknowledged. First, this study was mainly performed using overexpression systems in HEK293 cells, which may not fully reflect endogenous physiological conditions. Second, the study relied primarily on static imaging and biochemical assays, and therefore could not directly assess the real-time dynamics of TPL2-MEK1 trafficking. Third, although the findings support a scaffold-like role for TPL2, the precise mechanism underlying TPL2-mediated nuclear transport remains unclear. In addition, ubiquitination assays and proteasome inhibition experiments were not performed in this study, which limits

mechanistic understanding of TPL2 stability and degradation. Future studies using endogenous models, live-cell imaging, and transport-related mechanistic assays will be required to further validate these observations.

Acknowledgments

First and foremost, I would like to express my deepest gratitude to my supervisor, Dr. Ruaidhri Carmody, for his patience, encouragement, and invaluable guidance throughout my studies. Entering a new research field was initially challenging for me, but he always took the time to explain concepts step by step and constantly motivated me to move forward. During my most difficult financial period, he also helped me to apply scholarships. Meeting such a mentor has been one of the greatest fortunes in my life.

I would also like to thank Sara from the school's administrative office for her incredible patience and efficiency. She always responded to my numerous questions with kindness and care. My sincere thanks also go to the university security team, who often checked on me and kept me company during my late-night experiments, since I worked during the day and could only conduct experiments at night. Their concern and friendly conversations truly warmed my heart. I am also grateful to my second supervisor, Dr. Nathan, and Dr. Ian, for their generous support during my scholarship application, including writing recommendation letters and assisting with administrative procedures.

My heartfelt thanks extend to my dear friend Xinmeng, a PhD student in the School of Molecular Biosciences (SMB). Our buildings were close, and he became not only my best meal buddy but also the go-to person whenever I needed experimental advice. We shared long days, research frustrations, and laughter, which made academic life more joyful and less lonely. I am equally thankful to my labmates, including Nada, Assala and Daren, and especially to Nada herself, whose kindness and the Kunafa she made remain truly unforgettable.

During my studies, I also went through many challenges, including cross-border legal disputes, financial difficulties, and even a period when I could hardly afford my tuition fees. That time was truly tough, but it was also during those experiences that I met many kind people and learned how to stand on my own. I am especially

grateful to every cat and dog I have cared for as a pet sitter. They not only gave me a new source of income but also helped me rediscover the meaning of life. Often, it was their companionship that made me feel less alone.

I also acknowledge that AI-assisted tools, including ChatGPT, Quill Bot, and Deeply, were used during the writing and editing of this thesis to assist with translation and improve the fluency and clarity of the text. In addition, AI-assisted design tools were used in the creation of Fig1-3 which were subsequently reviewed and refined with BioRender.

To everyone who has supported and cared for me on this journey, thank you all. Without you, none of this would have been possible.

Table of content

List of graphs

List of tables

List of figures

1. Introduction

1.1 Rationale for investigating TPL2 in the regulation of MAPK localization.

Cancer is now widely recognized not merely as a disease of uncontrolled cell proliferation but as a multi-layered pathological process involving genetic mutations, disrupted signalling pathways, and dynamic interactions with the tumour microenvironment. Among the many oncogenic pathways, the mitogen-activated protein kinase (MAPK) cascade, particularly its ERK1/2 branch, plays a central role in regulating tumour cell proliferation, survival, and therapeutic resistance (Moon et al., 2021). While activating mutations in RAS and BRAF have been extensively characterized as major drivers of MAPK hyperactivation (Holderfield et al., 2014; Lito et al., 2013), the upstream regulators that control the spatial dynamics of this pathway remain comparatively underexplored. (Lailler et al., 2019; Moon et al.,2021).

TPL2 (MAP3K8), as an upstream oncogenic kinase, activates MEK1/2 through growth factor/cytokine stimulation. Previous studies have shown that TPL2 undergoes rapid degradation upon entering the nucleus (Collins et al., 2019), but its nuclear transport mechanism and functional significance in signal transduction remain unclear. In contrast, the subcellular localization of downstream ERK has been extensively studied: ERK's nuclear-cytoplasmic shuttling is tightly regulated by phosphorylation and transport factors, thereby determining signal duration and specificity (Khokhlatchev et al., 1998; Plotnikov et al., 2011). This suggests that spatial dynamics may represent a crucial layer in MAPK pathway signal regulation. Consequently, it is speculated that TPL2, as an upstream regulator, may also play a significant role in MAPK signal modulation through its own nuclear-cytoplasmic distribution pattern. Figure 1 illustrates a proposed model in which TPL2, beyond its canonical role as an upstream activator of MEK1/2, may also contribute to the

spatial regulation of MAPK signaling through interactions with MEK1 during nuclear-cytoplasmic trafficking. This putative mechanism suggests that TPL2 may influence signaling specificity and duration through regulation of subcellular localization.

To put this investigation within the context of the broader regulatory landscape of MAPK cascades, the following section summarizes the structure, oncogenic potential, and therapeutic targeting of the canonical ERK/MAPK signalling axis.

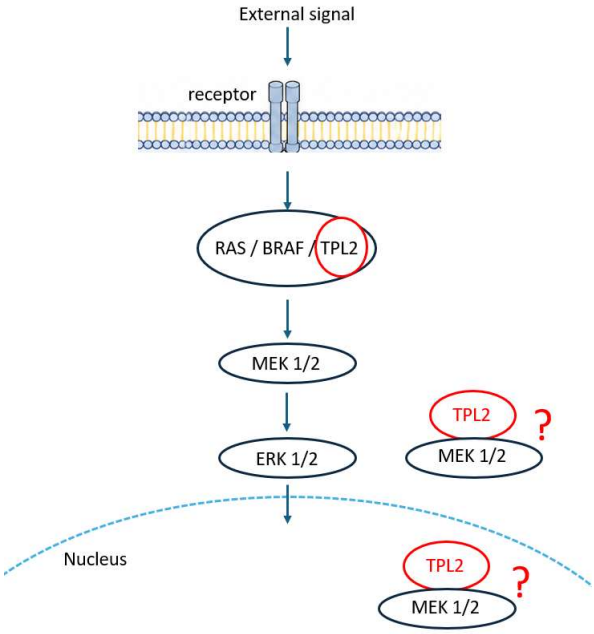

Figure 1. Proposed hypothesis of TPL involvement in MAPK signalling spatial regulation.

1.2 The ERK/MAPK signalling axis in oncogenesis and therapy

1.2.1 Structure and function of MAPK signalling

MAPK pathways are evolutionarily conserved signalling networks that translate a broad range of stimuli including growth factors, cytokines, or stress into distinct cellular responses. These three-tiered pathways consist of MAP3Ks phosphorylating and activating MAP2Ks, which then phosphorylate MAPKs and activate them to phosphorylate a variety of downstream substrates that can modulate proliferation, differentiation, survival, or cell death responses in the cell (Sebolt-Leopold et al., 2004).

Activation of MAPK pathways is typically initiated by signals from receptor tyrosine kinases (RTKs), G-protein coupled receptors (GPCRs), cytokine receptors, or other membrane-bound signaling molecules, which can lead to engagement of the Ras/Raf axis and subsequent activation of the MEK/ERK signaling cascade (Sundaram, 2006). In mammals, four major MAP kinase pathways are identified: ERK1/2, JNK, p38 and ERK5, which differ in their regulation and functions. Among the upstream MAP3Ks, TPL2 plays a unique role by directly phosphorylating MEK1, positioning it as a critical modulator within the ERK1/2 pathway. While ERK1/2 are mitogenic in nature, JNK and p38 are primarily activated by stress or inflammatory cues and promote apoptosis or differentiation (Ip and Davis, 1998; González et al., 1993). Signal crosstalk among these four MAPK pathways and feedback mechanisms regulate the outcome of the signal transduction in a context dependent manner (Plotnikov et al., 2011). Figure 2 shows the four major MAP kinase pathways.

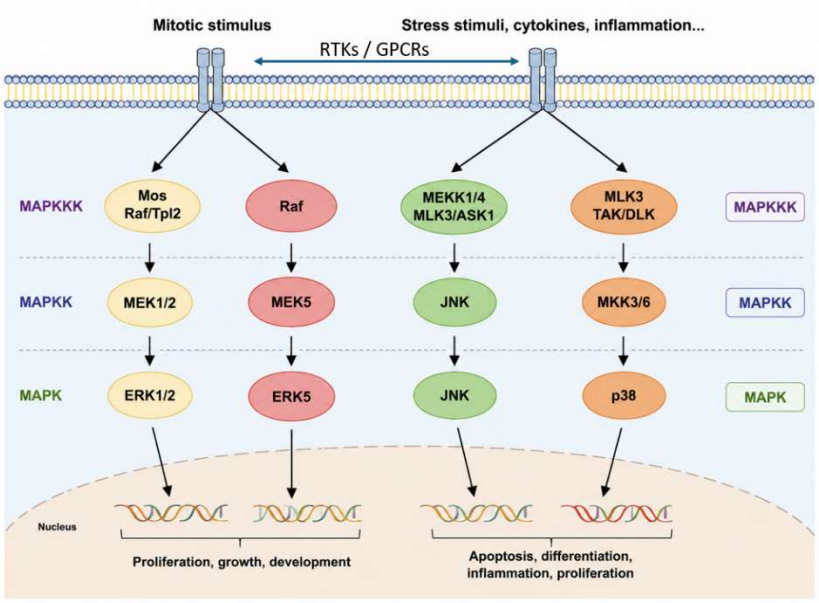

Figure 2. Schematic overview of the four major MAPK signalling pathways.

1.2.2 ERK pathway activation and oncogenic potential

Among the MAPK signalling pathways, the Ras/Raf/MEK/ERK cascade has been linked most frequently to cancer through its activation by growth factors like EGF (epidermal growth factor) (Holderfield et al., 2014; Lito et al., 2013). Activated Ras interacts with Raf, which phosphorylates MEK1, subsequently leading to activation of ERK1/2 (Sebolt-Leopold et al., 2004). ERK1/2 phosphorylates an array of substrates including transcription factors such as ELK1, c-fos, c-myc etc. Persistent activation of ERK1/2 has been shown to promote cell growth, angiogenesis, and anti-apoptotic mechanisms that can lead to oncogenesis (Lake et al., 2016). The role of ERK1/2 activation in cancer biology is underscored by frequent recurrent mutations observed in *KRAS* and *BRAF* genes in various malignancies (Barbacid et al.,1987). Aberrant activation of this cascade is a hallmark of many cancers. Mechanistically, feedback phosphorylation and Raf heterodimerization further shape the amplitude and duration of ERK1/2 signalling, and mutations in BRAF exploit these processes to sustain oncogenic ERK1/2 activation (Ritt et al., 2010). ERK1/2 activity is tightly regulated by its subcellular localization. Specific phosphorylation events control ERK1/2 nuclear import and shuttling, thereby influencing the duration and specificity of downstream signalling responses. (Khokhlatchev et al., 1998; Plotnikov et al., 2011). Understanding how upstream regulators, such as TPL2, influence ERK1/2 distribution is therefore vital.

1.2.3 Therapeutic targeting and resistance mechanisms

Given this central role of ERK1/2 pathway in cancer biology it has been pursued as a therapeutic target in cancer especially harbouring *BRAF* mutations. MEK1 inhibitors such as Trametinib, cobimetinib have shown clinical benefits and have been approved for therapeutic application (Flaherty et al., 2010) shown in Figure 3. However, the emergence of resistance phenotypes limits therapeutic response.

Mechanisms that lead to resistance include secondary mutations seen in RAS/RAF proteins, reactivation of ERK1/2 due to feedback compensatory mechanisms and

activation of alternative pro-survival pathways such as PI3K-AKT pathway (Wee et al.,2009; McCubrey et al.,2012). In addition, cancer cells can overcome pathway blockade through alteration in nuclear-cytoplasmic trafficking. For example, Plotnikov et al. (2011) showed that importin-7 mediated nuclear uptake of ERK1/2 regulates the intensity and duration of ERK1/2 signalling by facilitating access to nuclear substrates. Proposed strategies to address the escape phenomenon include targeting multiple nodes within the MAPK pathway, as well as pairing MAPK inhibitors with immune-modulating therapies (Ebert et al., 2016; Samatar et al., 2014). Of late, significant attention has been brought to upstream signalling mediators like TPL2 that can dictate subcellular localization pattern for MAPK induced signals under different contexts which holds promise for these strategies when implemented at clinical level.

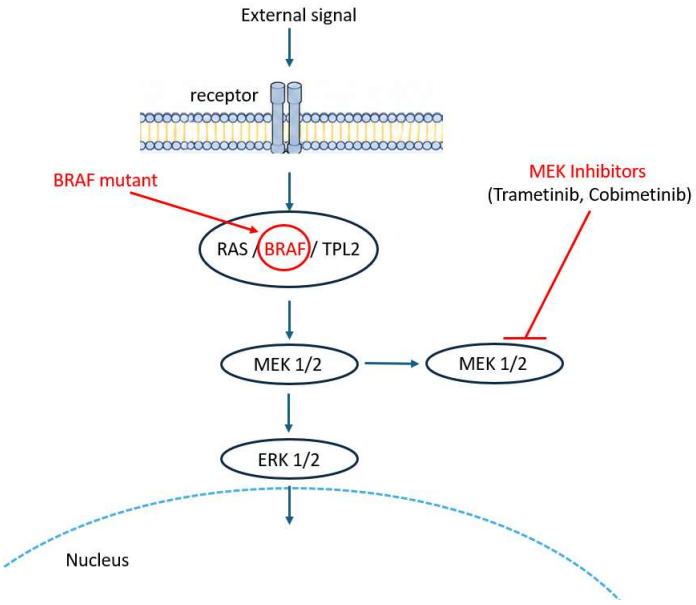

Figure 3. Therapeutic target through MAPK pathway.

BRAF mutations occur within the MAPK signaling pathway, and current therapeutic strategies (Trametinib and Cobimetinib) primarily focus on MEK inhibition.

1.3. TPL2 as an upstream modulator of ERK signalling.

1.3.1 Structural features and regulatory mechanisms of TPL2

TPL2 is a serine/threonine kinase located upstream of the MEK-ERK signalling pathway. TPL2 contains several regulatory regions that control its catalytic activity, subcellular localization, and stability. The protein exists in two isoforms, p58 and p52, which are produced by alternative translation initiation. The full-length isoform p58 is divided into three main regions: an N-terminal region (amino acids 11-30) containing a nuclear export signal (NES); a central kinase domain (amino acids 76-388); and a C-terminal region (amino acids 435-467) that includes a degron motif, several phosphorylation sites, and a putative PEST degradation sequence, which is considered a key element in the regulation of protein stability (Beinke et al., 2004; Lang et al., 2004).

Under basal conditions, TPL2 forms a trimeric complex together with the NF-κB1 precursor p105 and the adapter protein ABIN2. This complex keeps TPL2 in an inactive state and protects it from proteasomal degradation. Upon stimulation by pro-inflammatory cytokines such as TNF-α or IL-1β or by the activation of Toll-like receptors (TLR), IKKβ phosphorylates the p105 protein, leading to its partial proteasomal degradation. As a result, TPL2 is released and activated, phosphorylating MEK1/2 and initiating the ERK signalling cascade (Beinke et al., 2004).

The C-terminal region of TPL2 regulates both its catalytic activity and stability. It mediates the degradation of the protein via degron and PEST motifs. Deletion of this region significantly prolongs the half-life of TPL2 and increases the level of ERK1/2 phosphorylation, indicating a negative regulatory function. Several residues within this region, including S62, T290, and S400, are regulated by phosphorylation and modulate catalytic activity, thereby fine-tuning signal transduction (Robinson et al., 2007; Gantke et al., 2011). In contrast, a mutation of

D270A within the kinase domain results in a complete loss of TPL2 catalytic activity and is therefore frequently used to study the role of TPL2 in cellular signal transduction.

TPL2 is best known for its role in activation of MEK/ERK in the cytoplasm. However, recent findings suggest that TPL2 can also translocate to the nucleus under certain stress conditions. For example, following UVB-induced DNA damage, TPL2 enters the nucleus and phosphorylates histone H3 at Ser10, thereby initiating the expression of immediate early response genes such as c-Fos (Choi et al., 2008). Although the nuclear transport mechanism of TPL2 remains unclear, its structure contains motifs such as NES, PEST, and a putative degron. These elements are known to influence protein localization and stability in other systems. For example, NES mediates CRM1-dependent export (Kudo et al., 1998), PEST sequences promote proteasomal degradation (Rechsteiner and Rogers, 1996), and degrons act as ubiquitin-recognition signals (Varshavsky, 2011). While not yet validated in TPL2, the presence of these motifs suggests they may play similar regulatory roles. Investigating TPL2 mutants lacking these domains may provide insights into how TPL2 localization is controlled. Interestingly, the question arises as to whether MEK1 plays a role in this process. Given the close association between MEK1 and TPL2, it is possible that MEK1 facilitates or controls the translocation of TPL2 into the nucleus, revealing a new dimension of spatiotemporal regulation in the MAPK signalling pathway.

Figure 4 shows a schematic representation of the domain organization of TPL2 with the most important functional motifs and phosphorylation sites. These structural properties suggest that TPL2 acts as a dynamic, context-dependent regulator of the MAPK signalling pathway and can integrate inflammatory signals with proliferative signals in different subcellular compartments.

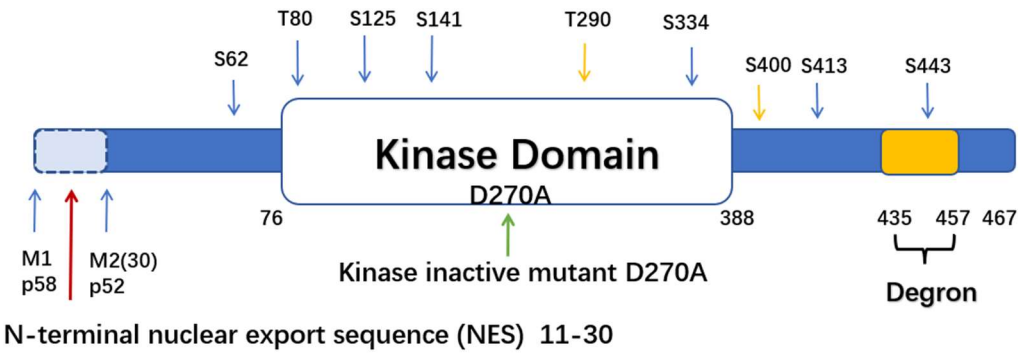

Figure 4. Domain organization and regulatory features of TPL2. This figure illustrates three distinct regions of TPL2: the N-terminal nuclear export sequence (NES; residues 11-30), the central serine/threonine kinase domain (residues 76-388), and the C-terminal degradation motif (residues 435-467). The C-terminal degradation motif (residues 435-467) contains a putative PEST degradation sequence, which is associated with protein degradation and turnover. Key phosphorylation sites are annotated as follows: S62, T80, S125, S141, T290, S334, S400, S413, and S443. The D270A mutation within the catalytic domain results in kinase inactivation. Two translation initiation codons, M1 and M2, generate the p58 and p52 isoforms, respectively. These structures, together with post-translational modification elements, jointly regulate TPL2 localization, stability, and kinase activity. Adapted from Xu et al. (2018).

1.3.2 Functional roles of TPL2 in cancer and inflammation

TPL2 is a central kinase at the intersection of inflammation, oncogenic signalling, and immune regulation. Although initially identified for its role in promoting innate immune responses downstream of Toll-like receptors (TLRs) and TNF receptors, increasing evidence suggests a broader involvement in cancer-associated inflammation and tumour progression (Xu et al., 2018; Njunge et al., 2020).

Figure 5 shows that TPL2 includes three functional axes that are coupled to each other: tumour-associated inflammation, carcinogenesis, and tumour immunity. In chronic inflammation, TPL2 activation facilitates the NF-κB and MAPK pathways, enhancing the synthesis of pro-inflammatory cytokines and chemokines. This is especially true for tumours that are caused by inflammation. Studies have shown that TPL2 (MAP3K8) is involved in tumour growth by changing how pro-inflammatory signals work, how cells grow, and how the immune system works. In hepatocellular carcinoma, TPL2 expression increases the NF-κB-dependent production of IL-6 and CCL2. This leads to more immunosuppressive macrophages getting into the tumour and creating a pro-tumour milieu (You et al., 2022). In colorectal cancer, TPL2 has been shown to play a role in promoting epithelial-mesenchymal transition (EMT) and cell proliferation via the MAPK pathway (Xia et al., 2021). It has been proposed that TPL2 decreases the sensitivity of cells to apoptosis and enhances stem cell-like traits (Wang et al., 2020; Hao et al., 2021). Recent studies have indicated that TPL2 is involved in remodelling immune cell infiltration and macrophage polarization during the development of tumorigenesis. In hepatocellular carcinoma (HCC), TPL2 has been shown to promote the infiltration of PD-L1-positive tumor-associated macrophages (TAMs), contributing to the formation of an immunosuppressive tumor microenvironment (You et al., 2022). Similarly in multiple myeloma, TPL2 promotes M2-like TAMS function to facilitate tumorigenesis and immune escape (Zhang et al., 2021). TPL2 might be involved in shaping the tumour immune microenvironment.

Additionally, a few studies have suggested that TPL2-regulated treatment-induced inflammatory response may confer tumour cell with adaptive drug resistance phenotypes. In melanoma, the expression level of TPL2 was significantly increased following BRAF inhibition treatment, which helps reactivate MEK/ERK signalling pathway and promote tumour cells survival during targeted therapy (Patel et al., 2021). Moreover, TPL2 was also involved in modulating the inflammatory response-associated treatment induced phenotypic plasticity in breast cancer, dynamic immune evasion of breast cancer cells from cytotoxic immune cells and acquisition of resistance to aromatase inhibitors (Hou et al., 2022). These studies suggest that TPL2 acts as a multifaceted oncoprotein that unifies treatment stressors, inflammatory responses, and immune checkpoint axis. Pharmacological or genetic blockade of TPL2 can induce apoptotic pressure on long-term survivor oncogenic driver pathways and modulation of the tumour microenvironment. (Lee et al., 2015).

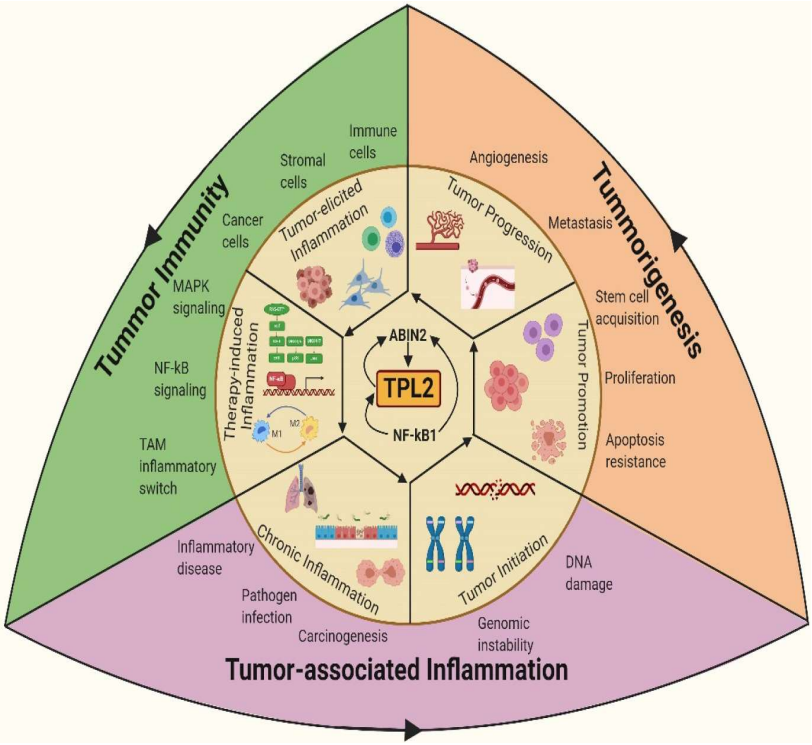

Graph 1. Multifaceted roles of TPL2 in inflammation, tumorigenesis, and tumour immunity.

This graph is adapted from Njunge et al., 2020 and illustrates that TPL2 plays a pivotal role in regulating signalling within the tumour microenvironment, orchestrating three primary functional axes: tumour-associated inflammation, carcinogenesis, and tumour immunity （Njunge et al.,2020）. In chronic inflammatory states, TPL2 is activated, creating a stable complex with NF-κB1 (p105) and ABIN2, which then activates the NF-κB/MAPK pathway, leading to the release of pro-inflammatory factors. This causes immune cells to change their programming, which starts the growth and spread of tumours. TPL2 can be reactivated by inflammation that lasts for a long time or gets worse in the microenvironment. This technique creates a loop of positive feedback: Inflammation activates TPL2, which causes tumours to grow. The tumour microenvironment keeps inflammation going, which makes the condition worse.

1.3.3 Nuclear localization of TPL2 and implications for MEK1-mediated regulation

TPL2 was initially believed to be a cytoplasm protein where it activates the MEK–ERK cascade. However, emerging evidence suggests that TPL2 can also translocate to the nucleus under stress conditions. Choi et al. (2008) observed that following UVB exposure in keratinocytes, TPL2 translocate to the nucleus and promotes the phosphorylation of histone H3 at serine 10 (Ser10), thereby augmenting the transcriptional activity of immediate early genes, including c-Fos. Collins et al. (2019) demonstrated that the nucleus-localized IκB-like protein BCL-3 regulates MAPK signaling by promoting the nuclear degradation of TPL2 via the ubiquitin–proteasome system, suggesting that TPL2 stability is tightly controlled in the nuclear compartment and may respond to stress or immune signals. They also identified an N-terminal nuclear export sequence (NES, aa 11-30) in TPL2 that mediates CRM1-dependent nuclear export, indicating that TPL2 localization is dynamically regulated through nuclear-cytoplasmic shuttling. Together these findings support the potential role of TPL2 in epigenetic regulation and suggest that its actions extend beyond traditional cytoplasmic pathways.

Previous studies have shown that components of the MAPK cascade, including MEK1, can localize to the nucleus and regulate function (Reiser et al.,1999). Although MEK1 lacks a classical nuclear localization signal (NLS), Chuderland et al., (2008) found that it can be recognized by Importin-7 through a phosphorylation-dependent nuclear transport signal (NTS) and go into the nucleus. In addition, MEK1 contains a leucine-rich nuclear export signal (NES) sequence, which allows it to be transported from nucleus via CRM1. Experiments by Adachi et al., (1999) showed that the selective CRM1 inhibitor Leptomycin B could significantly block the nuclear export of MEK1, further confirming that its nuclear export depends on the CRM1 pathway. These studies suggest that MEK1 may dynamically shuttle between the nucleus and cytoplasm under stress or kinase regulation, thus having

the potential to regulate the expression of nuclear target genes or protein interactions and playing a more complex role in tumour cell signalling. These nuclear import and export dynamics determine the subcellular localization of MEK1 and may also indirectly affect the localization of its binding partners, such as TPL2.

Recent studies have identified TRIM4 an E3 ubiquitin ligase, as a novel regulator of TPL2 stability. TRIM4 facilitates cytoplasmic degradation of TPL2 through K48- linked polyubiquitination (Bansod et al., 2024), thereby limiting sustained activation of the MEK-ERK pathway in KRAS-driven cancers. These findings were established using immunoprecipitation, ubiquitination assays, and CRISPR knockout models. Given that TPL2, MEK1 and TRIM4 all co-localise in the cytoplasm, it is plausible that TRIM4 may also indirectly affect MEK1 stability or localization, although this remains to be experimentally validated. Interestingly, TPL2 is also subject to nuclear regulation. For example, BCL-3, a nuclear IκB-like protein known to regulate inflammatory signaling pathways, was shown to mediate nuclear degradation of TPL2 through the ubiquitin-proteasome system (Collins et al., 2019). These findings suggest that TPL2 turnover is compartment-specific, with BCL-3 mediating nuclear degradation and TRIM4 promoting cytoplasmic degradation, indicating distinct mechanisms operating in different subcellular compartments.

In summary, current evidence indicates that TPL2 nuclear translocation may be modulated by several synergistic factors: (1) its interactions with MEK1; (2) BCL-3-mediated ubiquitin-proteasome regulation in the nucleus; (3) TRIM4-mediated ubiquitination in the cytoplasm. These regulatory mechanisms for subcellular localization may work together in MAPK signalling. This would then affect how precisely downstream genes are transcribed. Figure 5 gives an overview of this proposed model and its most important regulatory nodes.

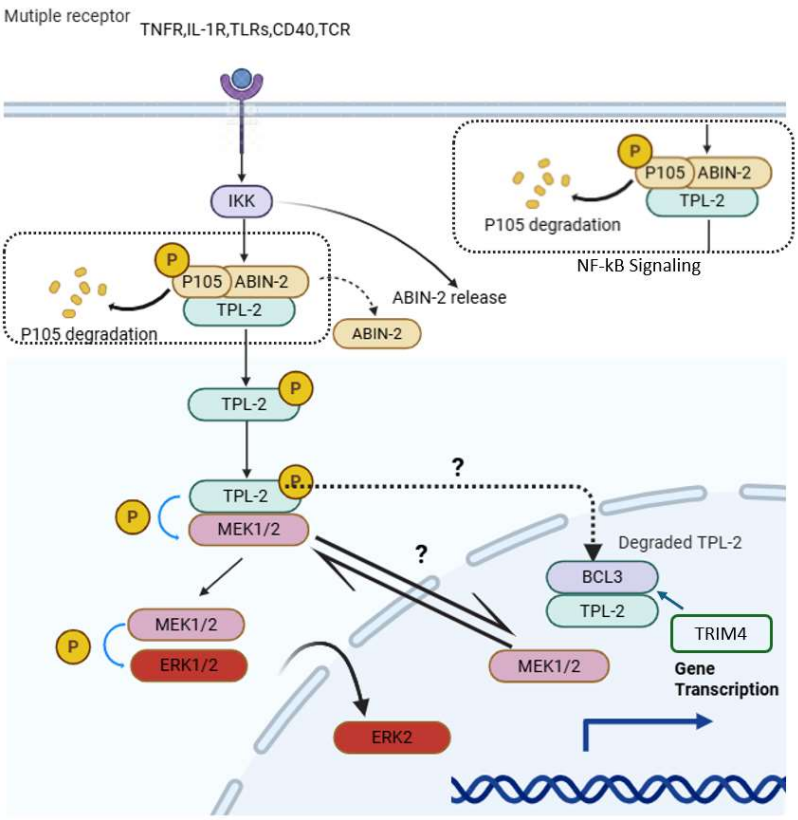

Figure 5. Proposed model of TPL2 nuclear translocation and degradation regulated by MEK1, BCL-3, and TRIM4.

This schematic illustrates a putative mechanism by which TPL2, traditionally cytoplasmic, can translocate into the nucleus and undergo compartment-specific regulation. Under proinflammatory stimuli (e.g., TNFR, IL-1R, TLRs), IKK-mediated phosphorylation of NF-κB1 p105 leads to its proteasomal degradation, releasing TPL2 from the inhibitory p105/ABIN-2 complex. Free TPL2 phosphorylates MEK1/2, activating the canonical MEK-ERK signalling cascade. In parallel, TPL2 may associate with MEK1/2 and translocate into the nucleus through a MEK1-mediated route. Once in the nucleus, TPL2 can be retained via interaction with BCL-3, a nuclear IκB family protein. This interaction may regulate nuclear dwell time and downstream transcriptional programs. Furthermore, the E3 ubiquitin ligase TRIM4 has been proposed to promote ubiquitin-dependent degradation of nuclear TPL2, potentially limiting its nuclear activity, requires further experimental validation. The exact signals and structural determinants that govern TPL2's nuclear entry and degradation remain to be fully elucidated.

1.4. Research gap and significance

The ERK/MAPK and its upstream protein TPL2 signalling pathway have been extensively studied. However, there is still a lack of research on the subcellular localization mechanism of TPL2 and a systematic discussion on its role as an upstream kinase in simultaneously regulating the stability and subcellular localization of MEK1. This thesis aims to study the blank in this aspect: (1) investigate the molecular mechanisms that control the nuclear-cytoplasmic shutting of TPL2; (2) examine hoe TPL2 regulates MEK1 localization and stability; (3) explore how these dynamic influence MAPK signalling and provide an experimental basis for the new treatment strategy for cancer.

2. Materials and Methods

All buffers used in the experiments below are detailed in the Buffer Table provided at the end of this section. Unless otherwise indicated, protease and phosphatase inhibitors were added fresh to buffers prior to use.

2.1 Cell culture and transfection

HEK293T and COS-7 cells were maintained in Dulbecco's Modified Eagle Medium (DMEM) supplemented with 10% fetal bovine serum (FBS), 2 mM L-glutamine, and 1% penicillin-streptomycin. Cells were grown at 37°C in a humidified atmosphere containing 5% CO_2. Cells were seeded into 6-well or 10-cm dishes and allowed to reach 70-80% confluency before transfection. For plasmid transfection, DNA was diluted in serum-free DMEM, and mixed with TurboFect reagent at a ratio of 1:2-1:3 (µg DNA: µL TurboFect). The mixture was incubated for 15 minutes at room temperature and added dropwise to the culture. Cells were harvested 24-48 hours post-transfection depending on the experimental purpose.

2.2 Plasmids and mutagenesis

A series of plasmids encoding human TPL2 and MEK1 were used in this study to investigate subcellular localization and kinase-dependent mechanisms. Several constructs were sourced from the laboratory collection. These included GFP-tagged wild-type TPL2 (GFP-TPL2^{WT}), a nuclear export signal deletion mutant (GFP-TPL2ΔNES), and a C-terminal truncation mutant (TPL2ΔC) tagged with FLAG. The wild-type MEK1 construct (MEK1^{WT}-MYC) was obtained from Addgene (Plasmid #40774).

Two new plasmids were constructed just for this project. The AAA-MEK1 mutant was designed based on a published sequence shown to disrupt MEK1 nuclear import (Chuderland et al., 2008). The AAA-MEK1 mutant was generated by replacing three threonine residues (T218, T222, and T226) within the nuclear transport signal (TPT motif) of MEK1 with alanine (T218A/T222A/T226A). These

residues are critical for phosphorylation-dependent importin-7 recognition and nuclear translocation. The resulting mutation alters the amino acid sequence from TPT to AAA in this region which impairs MEK1's nuclear import capacity. (Chuderland et al.,2008). The corresponding nucleotide codons were changed from ACC-CCC-ACC to GCC-GCC-GCC. The GFP-TPL2D270A was generated by substituting the aspartic acid (D) at position 270 within the TPL2 kinase domain with alanine (A), resulting in loss of kinase activity. The amino acid change corresponds to a codon change from GAC (Asp) to GCC (Ala). This mutant is commonly used to investigate the role of TPL2's catalytic function in cellular signal transduction. Both constructs were cloned into the pcDNA3.1 vector to facilitate subsequent immunoprecipitation (IP) assays. Detailed sequence information and construct features are provided in Table 1. This study used the Q5® site-directed mutagenesis kit to make all the mutations and deletions, and this experiment followed the manufacturer's instructions exactly. Table 1 shows the primers that were utilized for the mutation reaction. The generated plasmids were introduced into E. coli DH5α competent cells, and colonies were subsequently tested on LB agar plates supplemented with the appropriate antibiotics: ampicillin (100 μg/mL) for pcDNA3.1 constructs, and kanamycin (50 μg/mL) for pEGFP-based vectors. Qiagen micro-preparation, medium-preparation, or large-preparation kits were used to extract the plasmids according on the needs of the production. Sanger sequencing was utilized to check all the constructs. Table 2 has a full list of all the plasmids utilized in this work, together with thorough information about their vector backbone, epitope tag, antibiotic resistance, and mutation features.

2.3 Whole-cell protein extraction and subcellular fractionation

For whole cell lysate preparation, transfected cells were washed 3 times with 1ml cold phosphate-buffered saline (PBS) to remove residual medium. Cells were collected by centrifugation at 200 × g for 5 minutes at 4 °C, and the pellet was resuspended in 30-50 uL of cold RIPA buffer freshly supplemented with protease

and phosphatase inhibitors. After incubation on ice for 30 minutes with gentle mixing, lysates were clarified by centrifugation at 17000 × g for 10 minutes at 4°C. The resulting supernatants were collected and stored at -80 for immunoblotting or immunoprecipitation.

For subcellular fractionation, cytoplasmic and nuclear proteins were extracted using a modified protocol based on the Active Motif Nuclear Extract Kit. After collection and PBS washing, cells were pelleted and resuspended in 1×hypotonic buffer without vortexing and incubated on ice for 15 minutes. Subsequently, detergent was added to the suspension, followed by brief vortexing for 10 seconds. The mixture was centrifuged at 14,000 × g for 30s at 4 °C and carefully transferred cytoplasmic fraction to a new tube and stored at −80 °C.

The remaining nuclear pellet was then resuspended in complete nuclear lysis buffer and vortexed until fully dispersed. The suspension was incubated on ice for 30 minutes, with vortexing every 5 minutes to facilitate extraction. After a final 30-second vortex, the sample was centrifuged at 14,000 × g for 10 minutes at 4 °C. The resulting supernatant, containing the nuclear protein fraction, was transferred to a clean tube, and stored at −80 °C. All protein concentrations were determined using the BCA Protein Assay prior to downstream applications.

2.4 Western blotting

Protein concentration was measured using the BCA Protein Assay Kit (Thermo Fisher Scientific), following the manufacturer's protocol. Equal amounts of total protein (typically 10-50 μg per lane) were mixed with 2× SDS loading buffer and denatured by heating at 95 °C for 5 minutes.

The protein samples were separated by SDS-PAGE using 8-12% polyacrylamide resolving gels. Electrophoresis was performed at a constant voltage of 120 V for 90 minutes in running buffer. Following separation, the proteins were transferred onto

nitrocellulose (NC) membranes using a wet transfer system. The transfer was carried out at 100 V for 60 minutes in ice-cold transfer buffer.

Membranes were then blocked in 5% non-fat dry milk prepared in phosphate-buffered saline with 0.1% Tween-20 (PBST) for 1 hour at room temperature. For primary antibody incubation, antibodies were diluted in 5% bovine serum albumin (BSA) in PBST. Specifically, 5 g of BSA (Fraction V) was dissolved in 100 mL PBST, filtered through a 0.22 μm membrane, and stored at 4 °C for short-term use. Membranes were incubated with primary antibodies overnight at 4 °C.

After three washes in PBST (5 minutes each), membranes were incubated with secondary antibodies (1:5000 dilution in 5% non-fat dry milk) for 1 hour at room temperature. Protein bands were visualized using the LI-COR Odyssey imaging system, and signal intensities were quantified using ImageJ software.

Detailed compositions of all buffer solutions used in this procedure are listed in Table 3.

2.5 Immunoprecipitation

Cell lysates were prepared from either whole cell extracts or nuclear and cytoplasmic fractions, depending on experimental requirements. Protein concentration was quantified using the BCA assay, and equal amounts of lysate were subjected to immunoprecipitation as follows.

For each sample, lysates were combined with 0.5 μg of primary antibody and 25 μL of protein G magnetic beads (50% slurry), in a final volume of up to 1 mL RIPA buffer supplemented with freshly added protease and phosphatase inhibitors. The mixture was incubated overnight at 4 °C with gentle rotation.

On the following day, beads were pelleted by centrifugation at 8,000 × g for 10 seconds at 4 °C, and the supernatant was discarded. Beads were then washed three times with 1 mL of ice-cold RIPA buffer (without inhibitors), with each wash

performed by inverting the tubes 10 times on ice. After the final wash, beads were resuspended in 25 µL of 2× SDS loading buffer and boiled at 97 °C for 5 minutes.

Following heat denaturation, samples were vortexed for 10 seconds and centrifuged at 8,000 × g for 2 minutes at 4 °C. The supernatants containing immunoprecipitated proteins were collected and subjected to SDS–PAGE and immunoblotting.

2.6 Fluorescence and confocal microscopy

Transfected cells expressing GFP-tagged constructs were seeded onto sterilized glass coverslips in 6-well plates and incubated overnight under standard culture conditions. For live-cell imaging, cells were examined directly under an EVOS fluorescence microscope without fixation.

Fixation was performed using 4% methanol-free formaldehyde (prepared by diluting 16% stock solution at 3:1 with PBS) for 15 minutes at room temperature. After fixation, cells were washed again three times with PBS (5 minutes each).

Nuclei were stained with Hoechst 33342 (Thermo Scientific, Ref. 62249) at a final concentration of 1 µg/mL. Cells were incubated in the dark for 10 minutes at room temperature, followed by a PBS wash and transfer to fresh PBS for imaging.

Fluorescence images were acquired using either an EVOS microscope or a confocal laser scanning microscope at the institutional imaging facility.

2.7 Antibodies and dilution

A complete list of primary and secondary antibodies, their sources, and working dilutions used for Western blotting, immunoprecipitation, and immunofluorescence is provided in the Table 4 at the end of this section. Dilutions were optimized experimentally to minimize background and maximize signal specificity.

2.8 Statistical analysis

Quantitative data were analyzed using ImageJ and GraphPad Prism 9. Due to the preliminary nature of the study and limited experimental repeats, statistical

analysis was not performed, and the data are therefore presented descriptively without error bars.

2.9 List of tables

1. Primer table for Thesis

Target Construct	Template Plasmid	Primer Name	Sequence (5'→3')	Application & Target Region
AAA-MEK1	MEK1^{WT}-MYC (Addgene #40774)	AAA_primer_F	GCC CAG CGC AGC AGC CCA TGC TGC	Mutagenesis NTS triple alanine substitution
		AAA_primer_R	TGG TTA AGG CCG ATG GTG GAG C	Mutagenesis NTS triple alanine substitution
TPL2^{D270A}	GFP-TPL2^{WT} (lab stock)	Rella_MUT_A_F_hplc	TGT TTT GGT GGC TTT TGG CCT AAG	Mutagenesis Asp270 to Ala (D270A)
		Rella_MUT_A_R_hplc	GCT TTT GTG GAC ATG AAA AC	Mutagenesis Asp270 to Ala (D270A)
MEK1	MEK1^{WT}-MYC	Primer Biolab_F	AGC CCA TGC TGC TGG CGT CTA AC	Sequencing
MEK1	MEK1^{WT}-MYC	Primer Biolab_R	GCT GCG CTG GGC TGG TTA AGG CC	Sequencing
TPL2	GFP-TPL2^{WT}	pCMV_F	CGC AAA TGG GCG GTA GGC GTG	Sequencing
TPL2	GFP-TPL2^{WT}	EBV_R	GAT GAG TTT GGA CAA ACC AC	Sequencing

Table 1. Oligonucleotide primers used for site-directed mutagenesis and plasmid validation.

All primer sequences are written in the 5' to 3' orientation. The table includes primer names, corresponding template plasmids, and their functional applications. Primers labelled as mutagenesis primers were used to generate point mutations via site-directed mutagenesis using the Q5® High-Fidelity DNA Polymerase and a standard KLD (Kinase-Ligase-Dpnl) ligation protocol. Specifically, a triple alanine substitution was introduced into the MEK1 nuclear translocation signal (NTS; T218A, T222A, T226A) to generate the AAA-MEK1 construct, and an aspartic acid to alanine substitution (D270A) was introduced at position 270 of TPL2. Primers labelled as sequencing primers were used for plasmid validation by Sanger sequencing. They anneal to regions flanking the insert to confirm the integrity of both wild-type and mutant coding sequences. All mutant constructs were verified by Sanger sequencing using the indicated flanking primers.

2. Plasmid Table for Thesis

Plasmid Name	Backbone	Insert	Tag	Antibiotic	Source	Function / Notes
GFP-TPL2^{WT}	pEGFP	TPL2^{WT}	GFP	Kanamycin	Ruaidhri Carmody Lab	Wild-type TPL2 for subcellular localization studies
GFP-TPL2-ΔNES	pEGFP	TPL2 ΔNES	GFP	Kanamycin	Ruaidhri Carmody Lab	NES-deletion mutant to study nuclear export
GFP-TPL2^{D270A}	pEGFP	TPL2^{D270A}	GFP	Kanamycin	Constructed in this study	D270A point mutation in the kinase domain to inactive TPL2 kinase function
TPL2-FLAG	pcDNA 3.1	TPL2^{WT}	FLAG	Ampicillin	Ruaidhri Carmody Lab	Wild-type TPL2 for expression and IP
TPL2^{D270A} -MYC	pcDNA 3.1	TPL2^{D270A}	MYC	Ampicillin	Ruaidhri Carmody Lab	Kinase-dead TPL2 with MYC tag
TPL2ΔC-FLAG	pcDNA 3.1	TPL2 ΔC	FLAG	Ampicillin	Ruaidhri Carmody Lab	C-terminal truncation to study structure-function
MEK1^{WT}-MYC	pcDNA 3.1	MEK1^{WT}-MYC	MYC	Ampicillin	Addgene (MEK1 #40774)	Wild-type MEK1 purchased for control expression
AAA-MEK1-MYC	pcDNA 3.1	AAA-MEK1	MYC	Ampicillin	Constructed in this study	T218A/T222A/T226A triple mutant to study MEK1 nuclear localization

Table 2. Plasmid used in this thesis.

This table lists the plasmids used for expression and functional analysis of TPL2 and MEK1 variants. TPL2 constructs, including wild-type, NES-deletion (ΔNES), kinase-inactive(D270A), and C-terminal truncation (ΔC), were derived from existing lab stocks (Ruadhri Carmody Lab), except for GFP-TPL2^{D270A}, which was generated in this study. MEK1^{WT}-MYC was purchased from Addgene (Plasmid #40774), while the nuclear

translocation-defective mutant AAA-MEK1-MYC was created via site-directed mutagenesis in this study.

3. Buffer table for thesis

Buffer Name	Composition	Notes
RIPA Buffer	50 mM Tris-HCl (pH 7.4), 150 mM NaCl, 1% NP-40, 0.25% Sodium deoxycholate, 1 mM EDTA, 1 mM PMSF*, 2 µg/mL aprotinin*, 1 µg/mL pepstatin*, 2 µg/mL leupeptin*, 1 mM NaF*, 1 mM Na_3VO_4*	*Protease and phosphatase inhibitors added fresh on day of use
2X SDS Sample Buffer	100 mM Tris-HCl (pH 6.8), 4% SDS, 0.2% Bromophenol blue, 20% Glycerol, 200 mM β-mercaptoethanol	Used to elute protein from beads for SDS-PAGE
Wash Buffer (PBS)	137 mM NaCl, 2.7 mM KCl, 10 mM Na_2HPO_4, 1.8 mM KH_2PO_4, pH 7.4	Used to wash cells and beads
Running Buffer	25 mM Tris, 192 mM Glycine, 0.1% SDS	Used for SDS–PAGE electrophoresis
Transfer Buffer	25 mM Tris, 192 mM Glycine, 20% Methanol	Used cold with wet transfer system to transfer proteins to NC membranes

Table 3. Buffers used for cell lysis, immunoprecipitation, and immunoblotting.

This table summarizes the composition and specific functions of the buffer systems employed across key experimental procedures, including cell lysis, protein extraction, immunoprecipitation (IP), SDS–PAGE, and Western blotting (WB).

4. Antibody for this thesis

Target Protein	Primary Antibody (P)	Host	Vendor (Cat No.)	Dilution (P)	Secondary Antibody	Dilution (S)
TPL2-MYC	Anti-MYC	M	Santa Cruz (Sc-40)	1:1000	IRDye 800CW	1:5000
TPL2-FLAG	Anti-FLAG (DYKDDDDK)	M	GenScript (A00187)	1:5000	IRDye 800CW	1:5000
TPL2	Anti-TPL2 (E1R5H)	R	Cell Signaling Technology (#4174)	1:1000	IRDye® 680RD	1:5000
GAPDH	Clone 1E6D9	M	Proteintech (#60004-1-Ig)	1:50,000	IRDye 800CW	1:5000
p-ERK1/2 (Thr202/Tyr204)	Anti-Perk	R	Cell Signaling Technology (#9101)	1:5000	IRDye® 680RD	1:5000
MEK1	Anti-MEK1	M	Cell Signaling Technology (#4694)	1:1000	IRDye 800CW	1:5000

Table 4. Primary and secondary antibodies used for Western blotting.

This table lists the antibodies used in this study for immunoblotting. Primary antibodies were diluted in 5% BSA (bovine serum albumin) in PBST to preserve target epitope specificity, especially for phosphorylated proteins. Secondary antibodies conjugated with IRDye® 680RD or IRDye® 800CW (LI-COR Biosciences) were diluted in 5% non-fat milk in PBST. Membranes were scanned using the LI-COR Odyssey system under standardized imaging conditions for dual-channel detection (700 nm and 800 nm). GAPDH served as a loading control. M is mouse, R is rabbit.

3.Results

3.1 Plasmid construction and mutagenesis verification

To investigate the role of TPL2 kinase activity and MEK1 nuclear translocation in subcellular signalling, I constructed two expression plasmids: a kinase-dead mutant of TPL2 fused to GFP (GFP-TPL2^{D270A}), and a nuclear-translocation-deficient MEK1 mutant (AAA-MEK1), in which three threonine residues (T218, T222, and T226) in the conserved TPT motif were replaced with alanine.

Site-directed mutagenesis was performed using the Q5® High-Fidelity DNA Polymerase and a standard KLD (Kinase-Ligase-DpnI) protocol to introduce point mutations. The resulting products were transformed into chemically competent E. coli DH5α cells. After antibiotic selection on LB agar plates, well-grown single colonies were picked and cultured in LB medium. Plasmid DNA was extracted via mini-prep and analyzed by agarose gel electrophoresis to confirm successful transformation and assess plasmid integrity. As shown in Figure 6A-B, all clones yielded DNA of the expected size (~6 kb), although some smearing was observed. Clones with clear bands were selected for Sanger sequencing.

A.

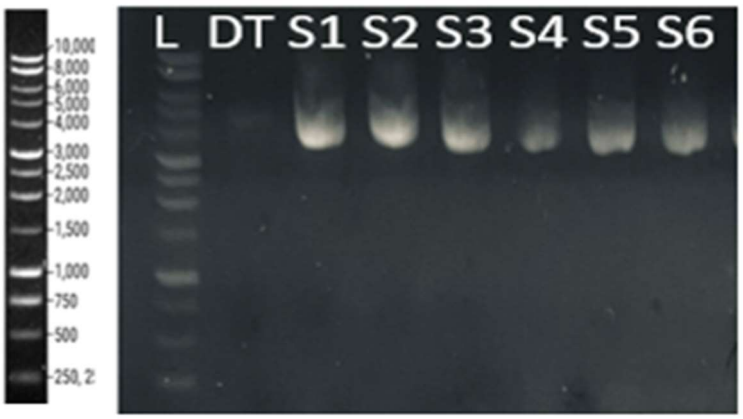
L DT S1 S2 S3 S4 S5 S6
10,000
8,000
6,000
5,000
4,000
3,000
2,500
2,000
1,500
1,000
750
500
250, 2

B.

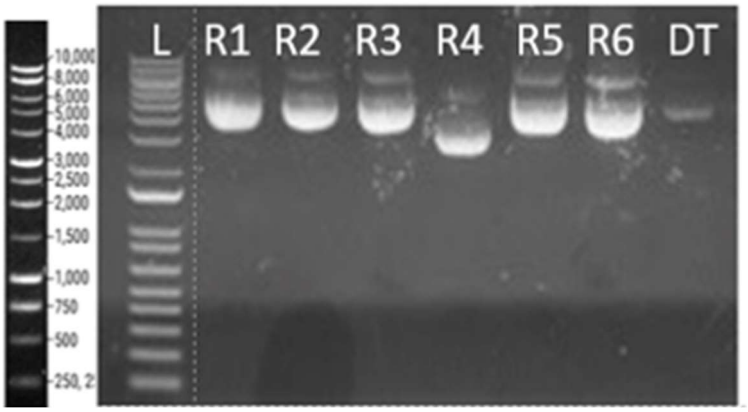
L R1 R2 R3 R4 R5 R6 DT
10,000
8,000
6,000
5,000
4,000
3,000
2,500
2,000
1,500
1,000
750
500
250, 2

C.

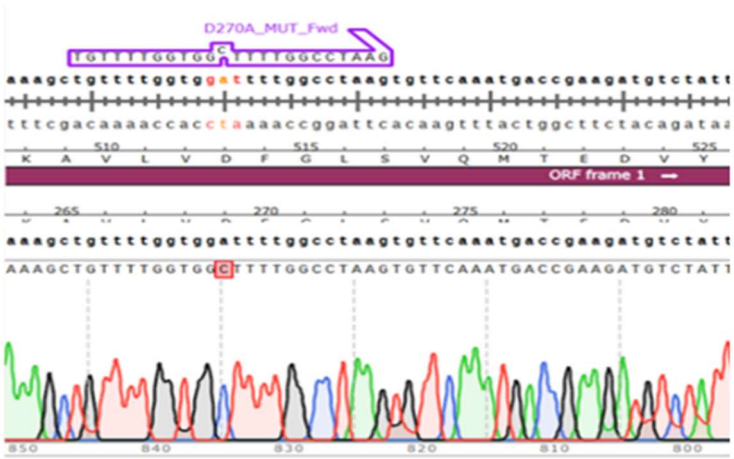
D270A_MUT_Fwd
ORF frame 1

D.

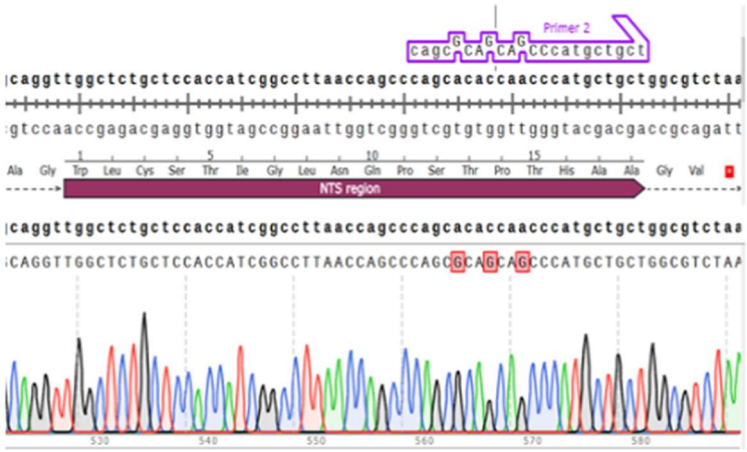
Primer 2
NTS region

Figure 6. Verification of GFP- TPL2^{D270A} and AAA-MEK1 mutant constructs by site-directed mutagenesis, PCR amplification, and Sanger sequencing.

(A, B) Plasmid DNA extracted from individual colonies (S1-S6 / R1-R6) was analysed by agarose gel electrophoresis. **(A)** GFP-TPL2^{D270A} plasmids yielded products of approximately 6 kb, aligning with the expected size of the full-length plasmid on a 1 kb Plus DNA Ladder (Biolab). Smearing was observed in multiple lanes, likely due to incomplete extension or partial template degradation. **(B)** AAA-MEK1 mutant plasmids displayed the anticipated band size (6 kb) without non-specific bands**. (C)** Sanger sequencing chromatogram confirming a G>C substitution at nucleotide 808 in the TPL2 coding sequence, resulting in the intended Asp270→Ala (D270A) amino acid change. No additional mutations were identified. **(D)** Sequencing validation of the AAA-MEK1 mutant. The TPT motif (Thr218, Thr222, Thr226) was successfully replaced by alanine, converting the wild-type MEK1 sequence WLCSTIGLNQRSTPTHAA to WLCSTIGLNQRSAAAHAA. Clean chromatogram peaks confirmed precise base editing with no off-target effects or background signal.

Sequencing subsequently identified the correctly mutated constructs. For GFP-TPL2^{D270A}, sequencing of clone S3 confirmed a G>C substitution at nucleotide 808, corresponding to the desired aspartate-to-alanine (D270A) amino acid change (Figure 6C). For AAA-MEK1, clone R3 was validated to contain the three intended alanine substitutions at threonine residues 218, 222, and 226 within the conserved TPT motif (Figure 6D). These correctly edited constructs were subsequently used in downstream subcellular localisation and protein-protein interaction experiments.

3.2 Subcellular localization of TPL2 is regulated by cell context, kinase activity, and NES motif.

To determine whether the kinase activity and nuclear export sequence (NES) of TPL2 regulate its subcellular distribution, I compared the localization of wild type, ΔNES, and D270A mutants, all fused to GFP. Two widely used cell lines, HEK293T and COS-7, were selected to evaluate the localization of wild-type TPL2 (GFP-TPL2^{WT}). As shown in Figure 7, HEK293T cells exhibited a diffuse GFP-TPL2^{WT} signal with minimal contrast between nuclear and cytoplasmic regions, limiting spatial resolution. In contrast, COS-7 cells showed a well-defined cytoplasmic localization pattern with clear exclusion from the nucleus, likely due to their flattened morphology and larger cytoplasmic area.

Subsequent imaging experiments were therefore performed in COS-7 cells due to their flat morphology and improved spatial resolution. These data demonstrate that the subcellular localization of the GFP-TPL2^{WT} protein is influenced by cellular characteristics, underscoring the significance of selecting an appropriate cell model for the study of protein dynamics. To investigate the mechanisms regulating TPL2's nuclear and cytoplasmic localization, two additional mutant constructs were assessed in COS-7 cells: a kinase-inactive variant (GFP-TPL2^{D270A}) and a mutant lacking the nuclear export signal (GFP-TPL2ΔNES). All the samples were imaged 24 hours after transfection in the same way (Fig. 8). The majority of GFP-TPL2^{WT} was in the cytoplasm, exhibiting a faint signal in the nucleus. This is consistent with other studies indicating that the protein remains in the cytoplasm through interactions with complexes such as NF-κB1/p105 and ABIN2 (Beinke and Ley, 2004).

The kinase-inactive mutant GFP-TPL2^{D270A} displayed weaker and more diffuse fluorescence throughout both the cytoplasm and nucleus, potentially reflecting reduced protein stability or altered subcellular trafficking. In contrast, GFP-

TPL2ΔNES showed pronounced accumulation in or around the nucleus, suggesting impaired nuclear export. Although a definitive nuclear export signal has not yet been mapped within TPL2, the nuclear enrichment observed upon NES deletion implies that active export is essential for maintaining its cytoplasmic distribution. While these localization patterns were generally reproducible, variability in fluorescence intensity and imaging quality limited quantitative analysis. Therefore, it remains unclear which structural feature predominantly governs TPL2 localization. The observed localization patterns, however, support the idea that TPL2 needs both kinase activity and an NES motif to be located to the cytoplasm.

To further evaluate the functional implications of these domains, I next assessed whether they also affect TPL2's interaction with MEK1 and its influence on MEK1 protein stability.

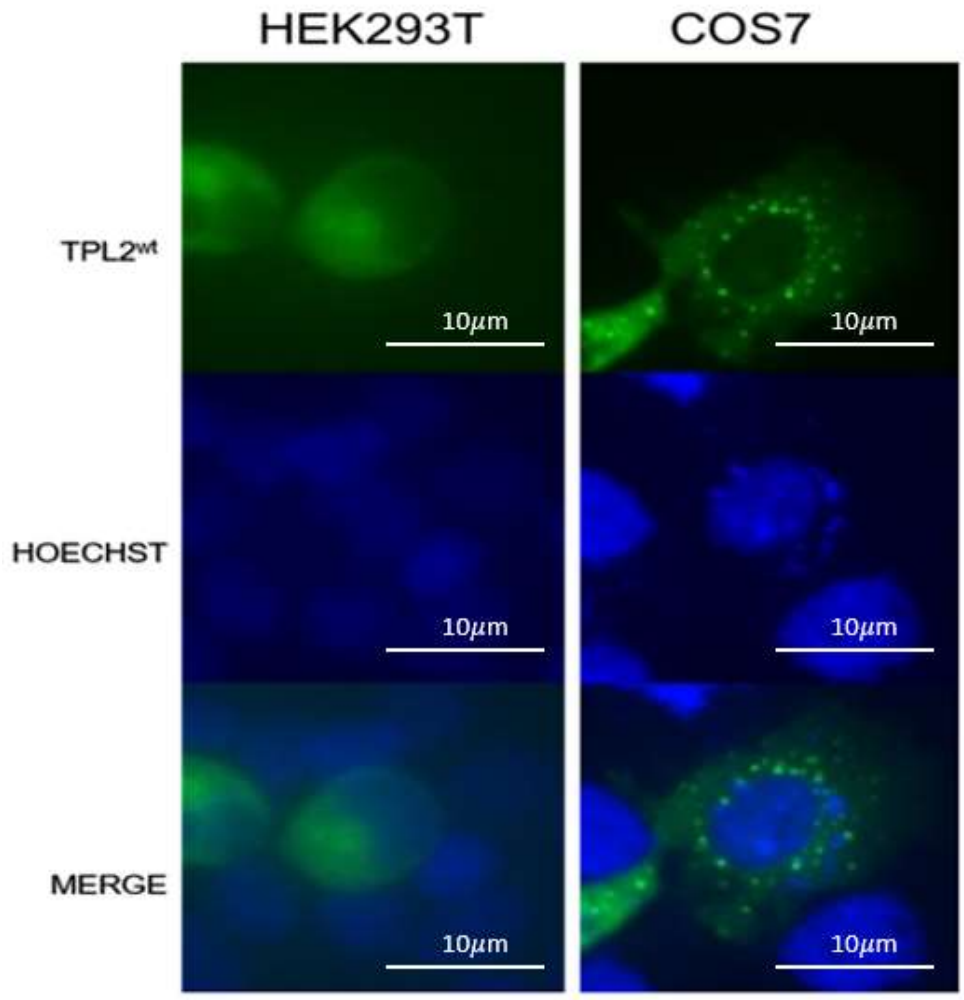

Figure 7. Subcellular Localization of GFP-TPL2 ^{WT} in HEK293T and COS-7 Cells

HEK293T and COS-7 cells were transfected with a GFP-TPL2^{WT} construct. Live cell imaging was conducted at 20× magnification using an EVOS fluorescence microscope twenty-four hours after transfection (Images were digitally magnified for improved visualization and presentation.). The GFP fluorescence in HEK293T cells was diffuse, with a lack of contrast between the nuclear and cytoplasmic regions. COS-7 cells exhibited a more distinct cytoplasmic localization, characterized by a faint signal in Hoechst-stained nuclei and a strong perinuclear accumulation. Due to my inconsistent cell culture techniques, the number of valid experimental images obtained was limited, and a considerable proportion of cells underwent death during imaging.

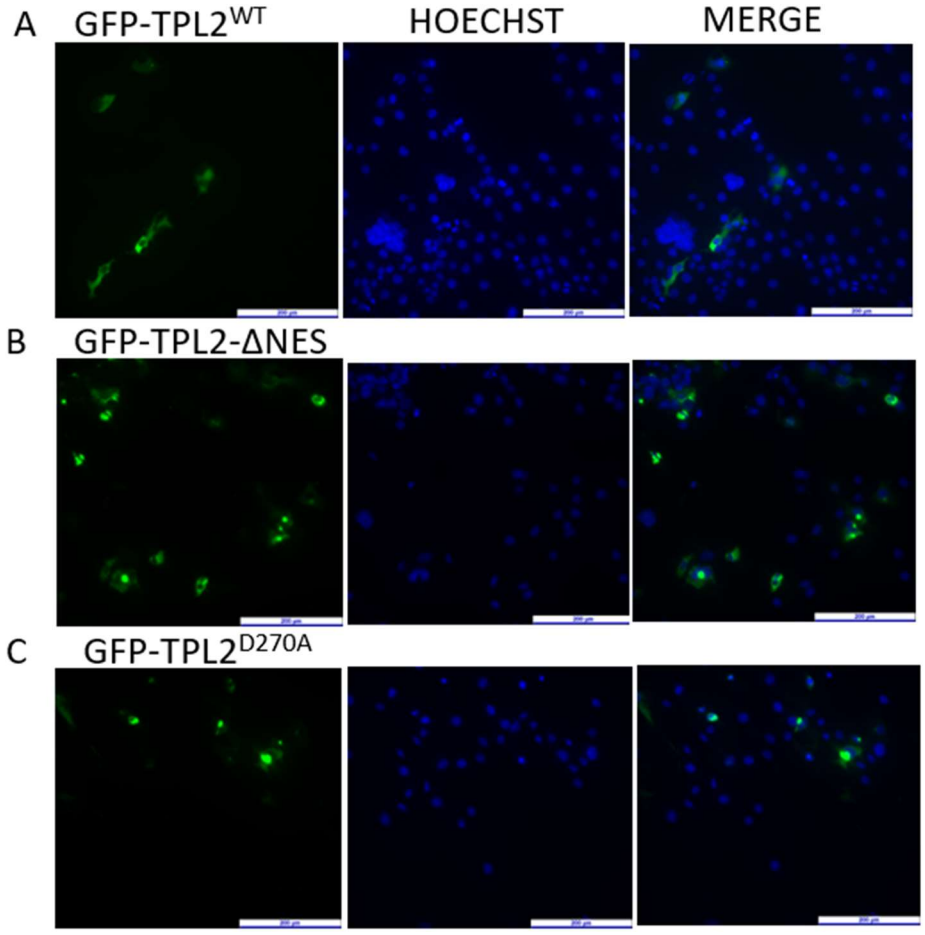

Figure 8. Subcellular localization of GFP-TPL2 variants in COS-7 cells.

COS-7 cells were transfected with GFP-tagged constructs that encoded either $TPL2^{WT}$, TPL2ΔNES, or $TPL2^{D270A}$. After 24 hours of transfection, the cells were fixated, the nuclei were visualized with Hoechst stain (blue), and the cells were imaged using fluorescence microscopy (GFP, green). (A) The cytoplasm was the primary location of $TPL2^{WT}$, and it was evidently excluded from the nucleus, which is consistent with the presence of a functional NES motif. (B) Deletion of the predicted NES in GFP-TPL2ΔNES resulted in perinuclear accumulation and partial nuclear enrichment in some cells, suggesting impaired nuclear export. However, the extent of nuclear localization varied between cells, possibly due to differences in expression level or imaging sensitivity. (C)$TPL2^{D270A}$ showed a more diffuse fluorescence pattern throughout both cytoplasm and nucleus, with partial nuclear accumulation. This distribution may indicate altered subcellular trafficking or impaired cytoplasmic anchoring due to loss of kinase activity. Although GFP signal intensity appeared comparable to the other constructs, its broader distribution contrasts with the more cytoplasm-restricted localization of GFP-$TPL2^{WT}$. The scale bar is 200 µm. Due to cell loss during the washing steps of the fixation procedure, although the experiments were repeated multiple times, the results were not consistently pronounced, and only one experiment produced particularly clear results.

3.3 TPL2-MEK1 interaction and its influence on MEK1 stability

The subcellular localization and stability of MAPK signalling components such as MEK1 are tightly controlled by upstream regulatory factors. Although TPL2 is best known for activating MEK1/ERK in inflammatory responses, the extent to which TPL2 structural features influence MEK1 protein abundance under basal conditions remains to be fully elucidated. To investigate this, we examined the physical association between TPL2 and MEK1 using immunoprecipitation (IP) assays and assessed whether different TPL2 variants affect steady-state MEK1 protein levels.

HEK293T cells were co-transfected with MEK1-MYC and either wild-type TPL2 ($TPL2^{WT}$) or a C-terminal truncation mutant (TPL2ΔC). Cells were collected and separated into cytoplasmic and nuclear fractions after 24 hours of transfection. First, Western blot was used to look at total protein to measure MEK1 protein levels in the steady state (Figure 9A). Co-transfection with TPL2ΔC consistently exhibited elevated MEK1 protein levels in the cytoplasmic fraction compared to $TPL2^{WT}$, indicating that the C-terminal structure of TPL2 may negatively regulate MEK1 stability. To confirm the protein-protein interaction between MEK1 and TPL2, immunoprecipitation of MEK1 was conducted using an anti-Myc antibody, followed by the detection of overexpressed TPL2 in the co-precipitated samples (Figure 9B). The results indicated weak binding signals for TPL2 in the cytoplasmic fraction, with negligible signals observed in the nuclear fraction. This could be because nuclear MEK1 levels are low or because immunoglobulin heavy chains get in the way during the co-immunoprecipitation process. The observed non-specific bands are likely derived from the IgG heavy chain (~50 kDa) and light chain (~25 kDa) of the anti-Myc antibody used during immunoprecipitation, which may partially obscure weak target-specific signals. These data demonstrate that MEK1 physically associates with TPL2 in the cytoplasm. Qualitatively, TPL2ΔC appeared to exhibit stronger co-precipitation with MEK1 compared to TPL2WT; however, due to signal variability, background interference, and the presence of IgG heavy and light chain bands, no reliable quantitative analysis could be performed for this

experiment, further supporting a role for the C- terminal region in modulating interaction strength. This observation led us to hypothesize that TPL2 structure may regulate MEK1 stability or localization, which was subsequently tested in later experiments.

A

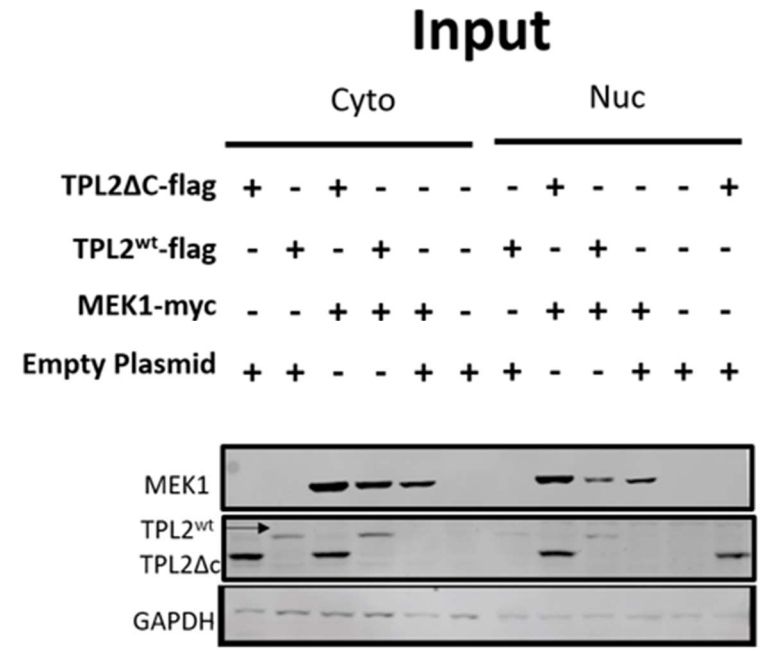
Input
Cyto
Nuc
TPL2ΔC-flag + - + - - - - + - - - +
TPL2wt-flag - + - + - - + - + - - -
MEK1-myc - - + + + - - + + + - -
Empty Plasmid + + - - + + + - - + + +
MEK1
TPL2wt
TPL2Δc
GAPDH

B

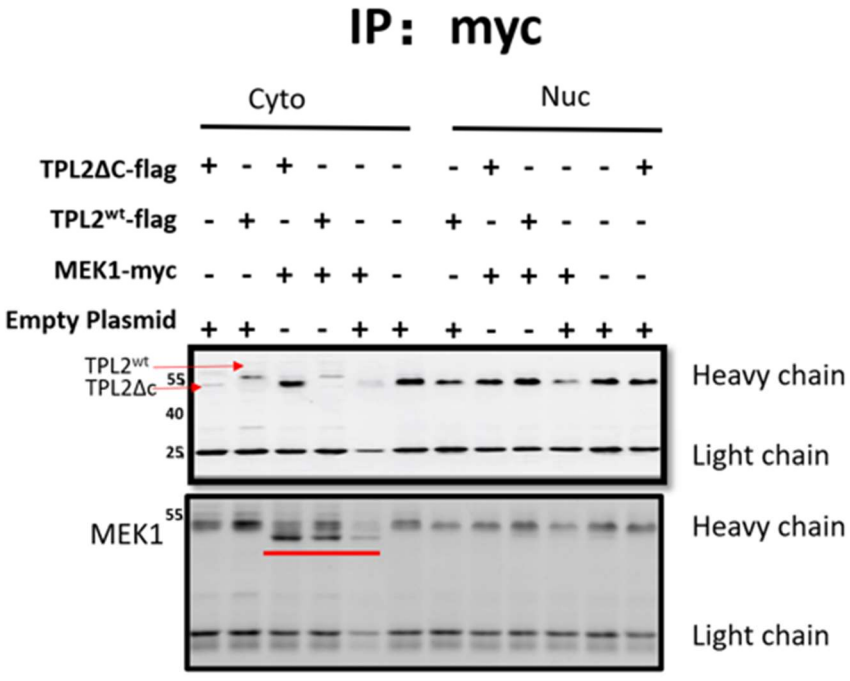
IP: myc
Cyto
Nuc
TPL2ΔC-flag + - + - - - - + - - - +
TPL2wt-flag - + - + - - + - + - - -
MEK1-myc - - + + + - - + + + - -
Empty Plasmid + + - - + + + - - + + +
TPL2wt
TPL2Δc
55
40
25
Heavy chain
Light chain
MEK1
55
Heavy chain
Light chain

Figure 9. Immunoprecipitation reveals differential interactions between MEK1 and TPL2 variants in cytoplasmic and nuclear compartments.

(A) Input controls for immunoprecipitation. HEK293T cells were co-transfected with MEK1-MYC and either FLAG-TPL2^{WT} or a truncated FLAG-TPL2ΔC construct (amino acids 1–399). 24 hours post-transfection, cells were fractionated into cytoplasmic and nuclear extracts. Western blot analysis confirmed expression of MEK1 and both TPL2 variants, with GAPDH used as a compartmental control. TPL2^{WT} and TPL2ΔC were both detected predominantly in the cytoplasmic fraction, although higher levels of TPL2ΔC were also observed in the nucleus. (B) Immunoprecipitation (IP) was performed using anti-MYC antibodies to isolate MEK1-associated complexes from both cytoplasmic and nuclear fractions. Immunoblotting with anti-FLAG revealed that both TPL2^{WT} (indicated by the first red arrow in the upper blot) and TPL2ΔC (second red arrow) could be pulled down with MEK1 in the cytoplasm. However, TPL2ΔC showed a noticeably stronger IP signal, suggesting a more stable or abundant interaction. In the nuclear fraction, TPL2^{WT} and TPL2ΔC were barely detectable in MEK1 immunoprecipitants. MEK1 was efficiently immunoprecipitated in the cytoplasm but barely seen in the nuclear fraction. The red horizontal line in the lower blot marks the position of MEK1, highlighted to distinguish it from overlapping heavy and light chain signals. Although no quantification was performed due to signal variability and background interference, the qualitative differences observed in this experiment provided preliminary insights that informed the design of subsequent experiments. Due to my inconsistencies in experimental technique, only one experiment produced valid results.

Due to the presence of heavy and light chain bands from the IP, the red marker highlights the specific location of MEK1. No quantification was performed for this experiment due to signal variability and background, but the qualitative differences provided initial insights that guided the design of subsequent experiments.

To investigate the effects of different TPL2 mutations on MEK1 protein expression levels, HEK293T cells were transfected with either the MEK1 alone, or co-transfected with $TPL2^{WT}$, TPL2ΔC, or $TPL2^{D270A}$. Cellular lysates were harvested 24 hours post-transfection for Western blot analysis (Figures 10A and 10C).

Compared to MEK1 expressed alone, co-expression with $TPL2^{WT}$ resulted in a modest increase in MEK1 protein levels, suggesting that wild-type TPL2 may slightly contribute to the stabilization of MEK1. Notably, co-transfection with TPL2ΔC, led to a markedly higher MEK1 expression than the TPL2WT group (Figures 10A). Importantly, the increased MEK1 levels in the TPL2ΔC group cannot be solely attributed to higher expression of TPL2ΔC itself, as the expression levels of TPL2ΔC and $TPL2^{WT}$ were comparable (Figure 10A), supporting a structural role for the C-terminal region in regulating MEK1 stability. This suggests that the C-terminal region of TPL2 may contain regulatory elements related to MEK1 degradation, and that its deletion increases MEK1 stability. Conversely, co-transfection with the kinase inactive mutant $TPL2^{D270A}$ did not increase MEK1 levels and instead resulted in slightly lower MEK1 expression compared to the $TPL2^{WT}$ co-transfection group (Figure 10C). This indicated that the kinase activity of TPL2 also plays a crucial role in the stability of MEK1. Therefore, these observations were considered preliminary and were used primarily to guide the design of subsequent experiments, and that its deletion increases MEK1 stability. Conversely, co-transfection with the kinase inactive mutant $TPL2^{D270A}$ did not increase MEK1 levels and instead resulted in slightly lower MEK1 expression compared to the $TPL2^{WT}$ co-transfection group (Figure 10C). This indicated that the kinase activity of TPL2 also plays a crucial role in the stability of MEK1.

Subsequently, a grayscale analysis of Western blot bands was performed using ImageJ software, normalizing the expression levels of MEK1 and TPL2 to GAPDH as an internal control (Figures 10B and 10D). Quantitative results confirmed the immunoblotting observations: MEK1 expression was highest in the TPL2ΔC co-transfection group, followed by the $TPL2^{WT}$ group, while MEK1 expression in the $TPL2^{D270A}$ group was approximately equal to that of the control group. This suggests that TPL2 influences the stability of the MEK1 protein through a dual mechanism involving both the C-terminal structure and kinase activity.

A

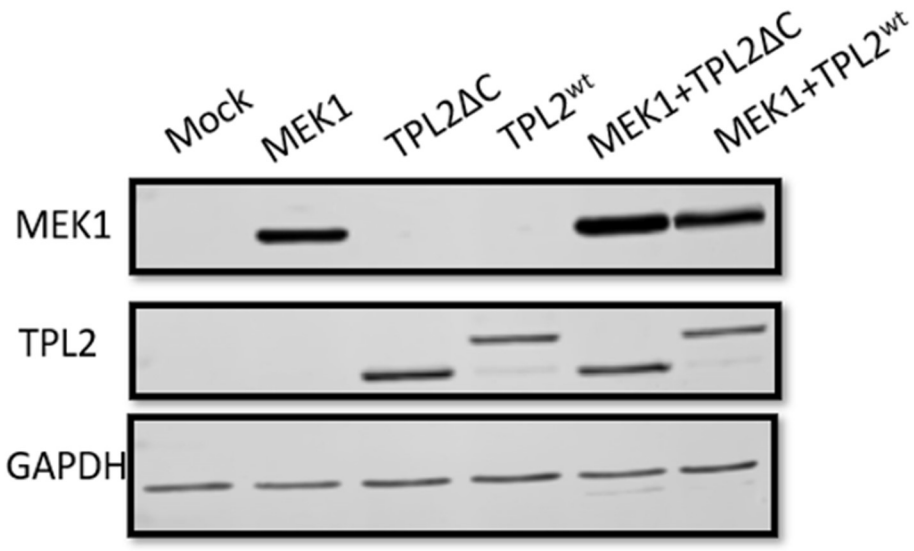
Mock
MEK1
TPL2ΔC
TPL2wt
MEK1+TPL2ΔC
MEK1+TPL2wt
MEK1
TPL2
GAPDH

B

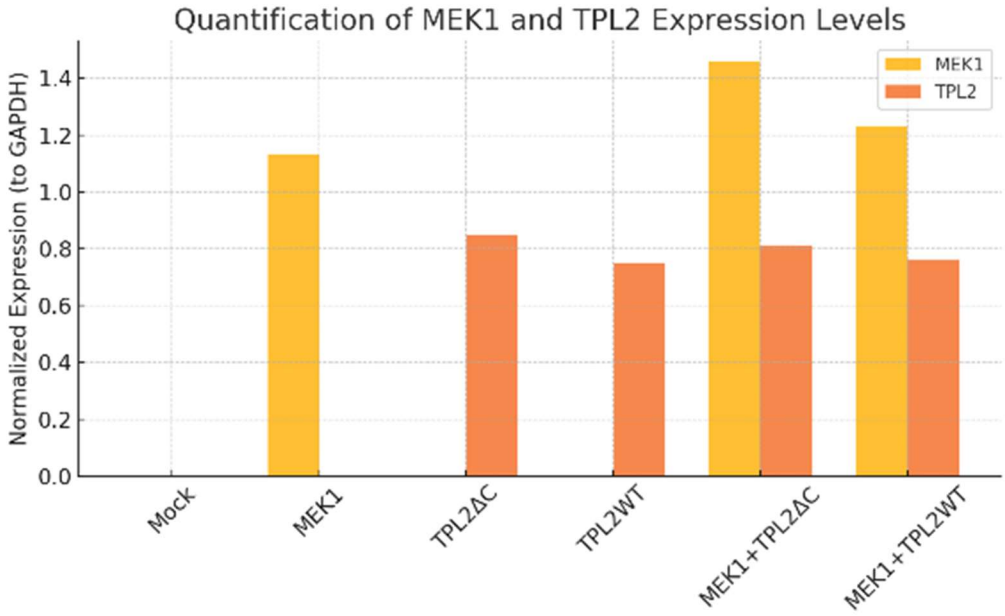
Quantification of MEK1 and TPL2 Expression Levels
Normalized Expression (to GAPDH)
0.0
0.2
0.4
0.6
0.8
1.0
1.2
1.4
MEK1
TPL2
Mock
MEK1
TPL2ΔC
TPL2WT
MEK1+TPL2ΔC
MEK1+TPL2WT

C

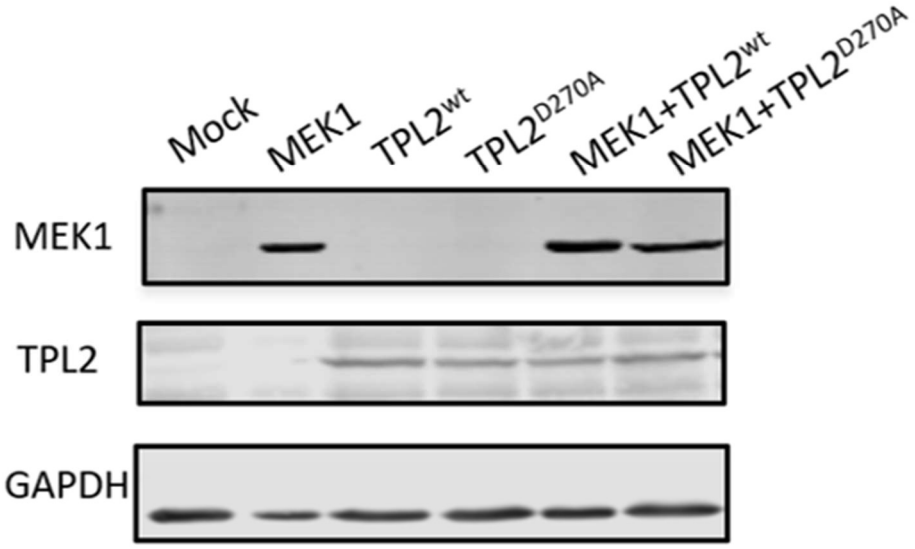
Mock
MEK1
TPL2wt
TPL2D270A
MEK1+TPL2wt
MEK1+TPL2D270A
MEK1
TPL2
GAPDH

D

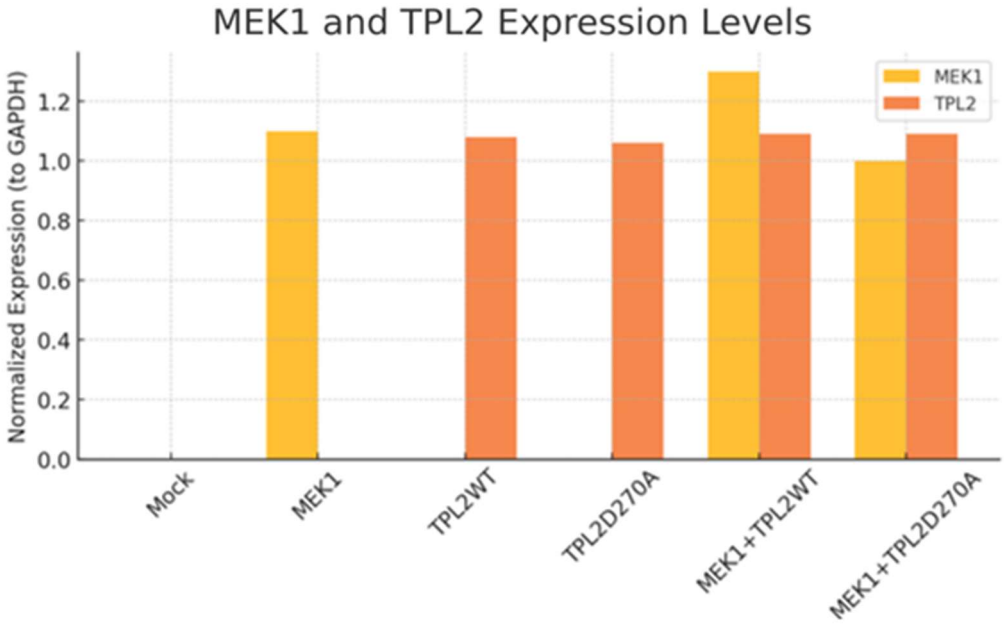
MEK1 and TPL2 Expression Levels
Normalized Expression (to GAPDH)
0.0
0.2
0.4
0.6
0.8
1.0
1.2
MEK1
TPL2
Mock
MEK1
TPL2WT
TPL2D270A
MEK1+TPL2WT
MEK1+TPL2D270A

Figure 10. TPL2 structural and catalytic integrity affects MEK1 expression levels.

(A) Western blot analysis of HEK293T cells transfected with MEK1-MYC, FLAG-TPL2ΔC (C-terminal truncation, aa1-399), or FLAG-$TPL2^{WT}$, individually or in combination. Cell lysates were harvested 24 hours post-transfection. Expression of MEK1 and TPL2 was assessed using anti-MYC and anti-FLAG antibodies, respectively. GAPDH served as the loading control. Co-expression of MEK1 with truncated TPL2ΔC resulted in a noticeable increase in MEK1 signal compared to MEK1 alone or co-transfection with full-length $TPL2^{WT}$. (B) Quantification of MEK1 and TPL2 protein levels from panel A. Relative band intensities were normalized to GAPDH and expressed relative to MEK1-only conditions. Co-expression with TPL2ΔC enhanced MEK1 protein abundance, suggesting that the C-terminal truncation may increase MEK1 stability or reduce degradation. (C) Western blot analysis of HEK293T cells transfected with MEK1–MYC and either FLAG-$TPL2^{WT}$ or a kinase-inactive mutant MYC-$TPL2^{D270A}$. As shown, co-expression of $TPL2^{WT}$ with MEK1 elevated MEK1 protein levels, whereas $TPL2^{D270A}$ failed to do so despite being expressed at comparable or higher levels. This suggests that TPL2 kinase activity contributes to MEK1 stabilization. (D) Quantification of MEK1 and TPL2 levels from panel C. Relative band intensities were normalized to GAPDH. Both $TPL2^{WT}$ and $TPL2^{D270A}$ were expressed at similar levels (≈1.1-fold relative to GAPDH), while only $TPL2^{WT}$ enhanced MEK1 protein abundance. This confirms that TPL2 catalytic activity, rather than its expression level, is required for MEK1 stabilization. No statistical analysis was performed due to limited repeats.

3.4 TPL2 alters the nuclear localization of the AAA-MEK1 mutant.

This study constructed a AAA-MEK1 mutant to further investigate the role of TPL2 in controlling the subcellular localization of MEK1, particularly under conditions where nuclear absorption of MEK1 is impaired. This mutation resulted in an alanine substitution at the Thr-Pro-Thr (TPT) phosphorylation site of MEK1, disrupting the non-canonical nuclear translocation signal.

HEK293T cells were transfected with plasmids encoding wild-type MEK1, AAA-MEK1, $TPL2^{WT}$, or combinations thereof. After 24 hours post-transfection, cells were fractionated into cytoplasmic and nuclear components, followed by Western blot analysis. GAPDH and HDAC1 were used as loading controls for cytoplasmic and nuclear fractions, respectively (Figure 11). As expected, AAA-MEK1 was predominantly detected in the cytoplasmic fraction, confirming its impaired nuclear localization. However, upon co-expression with $TPL2^{WT}$, AAA-MEK1 also became detectable in the nuclear fraction. This redistribution was specific to the AAA-MEK1 plus $TPL2^{WT}$ condition and was not observed with MEK1 alone or with wild-type MEK1 co-expressed with $TPL2^{WT}$. These results suggest that $TPL2^{WT}$ promotes nuclear accumulation of AAA-MEK1 despite its deficient nuclear localization signal. $TPL2^{WT}$ itself showed low but detectable presence in the nuclear fraction, supporting the idea that it may assist in the translocation of MEK1 into the nucleus through protein–protein interaction, as previously suggested in studies on the TPL2's ability to influence localization and stability of associated signalling partners (Breyer, 2020).

In summary, this study suggested a paradigm in which TPL2 not only controls how stable MEK1 is (see section 3.3), but also how it is localized in cells. In conditions of $TPL2^{WT}$ co-transfection, AAA-MEK1 demonstrates significant nuclear enrichment, even in the absence of intrinsic nuclear transport capability. This

indicates that TPL2 may promote MEK1 nuclear translocation through a piggyback mechanism.

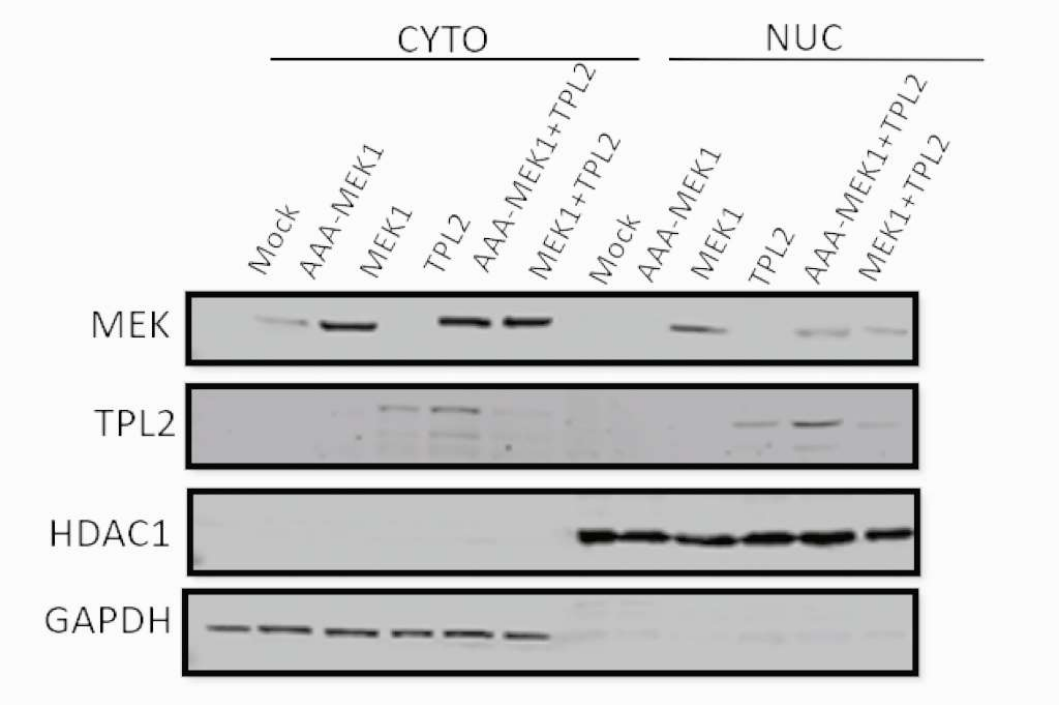

Figure 11. TPL2 promotes nuclear localization of the AAA-MEK1 mutant in HEK293T cells.

HEK293T cells were transfected with MEK1, AAA-MEK1, TPL2, or combinations thereof. After 24 hours, cells were separated into nuclear (NUC) and cytoplasmic (CYTO) fractions. Immunoblotting was performed for MEK1, TPL2, HDAC1 (nuclear marker), and GAPDH (cytoplasmic marker). AAA-MEK1 is retained in the cytoplasm unless co-expressed with TPL2, in which case it becomes detectable in the nucleus. Representative blot from one independent experiment.

3.5 C-terminal truncation of TPL2 enhances MEK1 expression and downstream ERK activation.

To investigate whether the C-terminal region of TPL2 affects its ability to regulate MEK1 expression and downstream signalling, we compared the effects of $TPL2^{WT}$ and TPL2ΔC on MEK1 abundance and ERK activation.

HEK293T cells were transfected with MEK1, $TPL2^{WT}$, TPL2ΔC, or combinations thereof. After 24 hours, whole-cell lysates were collected and analysed by Western blot for MEK1, TPL2, phosphorylated ERK (P-ERK), and GAPDH as a loading control (Figure 12A). The Western blot results were grayscale analysis by ImageJ software and normalized with GAPDH as the internal control, as shown in Figure 12B.

Western blot analysis showed that in cells co-transfected with MEK1 and TPL2ΔC, MEK1 protein levels were substantially higher than in cells co-transfected with MEK1 and $TPL2^{WT}$ or MEK1 alone. This suggests that removing the C-terminal domain of TPL2 may make it better at stabilizing MEK1. Furthermore, the co-expression of MEK1 with TPL2ΔC resulted in a further increase in MEK1 levels, although a modest enhancement was observed when co-expressed with $TPL2^{WT}$. Consistent with the elevated MEK1 levels, phosphorylated ERK (P-ERK) exhibited a substantial rise in the MEK1+TPL2ΔC co-transfection group. $TPL2^{WT}$ expression promoted ERK phosphorylation to some extent, but this effect was markedly amplified in TPL2ΔC conditions. These results suggest that the C-terminal domain of TPL2 may serve as a negative regulator of MEK1 stability and the subsequent activation of the ERK pathway.

A

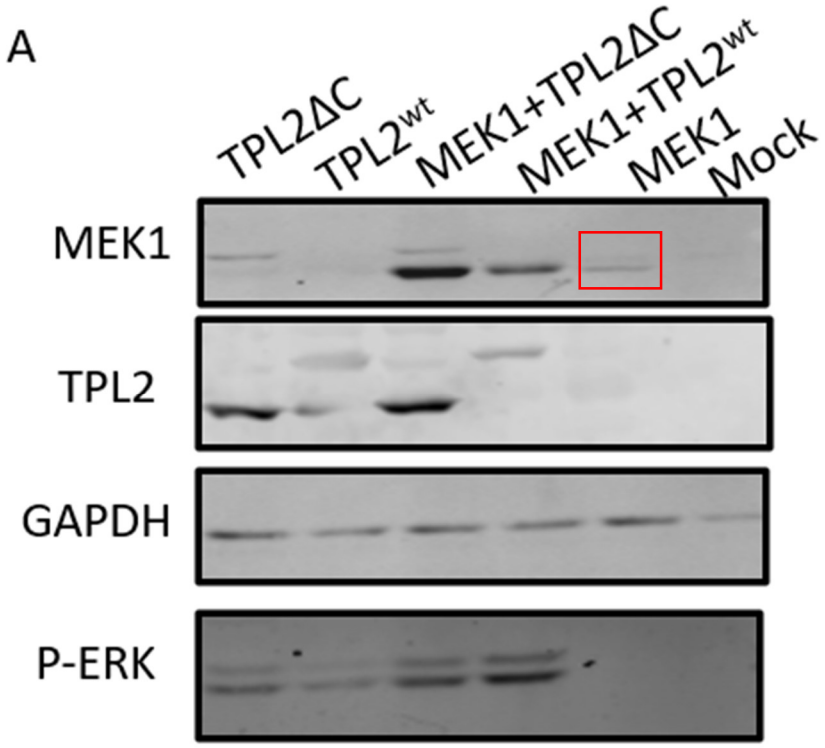
TPL2ΔC
TPL2wt
MEK1+TPL2ΔC
MEK1+TPL2wt
MEK1
Mock
MEK1
TPL2
GAPDH
P-ERK

B

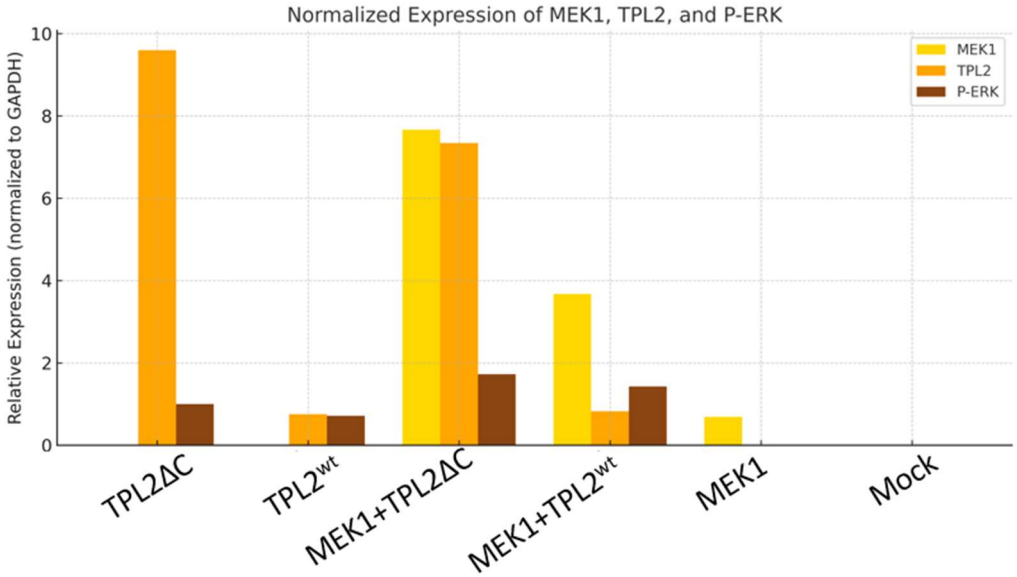
Normalized Expression of MEK1, TPL2, and P-ERK
Relative Expression (normalized to GAPDH)
MEK1
TPL2
P-ERK
0
2
4
6
8
10
TPL2ΔC
TPL2wt
MEK1+TPL2ΔC
MEK1+TPL2wt
MEK1
Mock

Figure 12. Truncated TPL2 enhances MEK1 stability and ERK activation in HEK293T cells.

(A) Western blot examination showed that in HEK293T cells that had been transfected with MEK1, $TPL2^{WT}$, TPL2ΔC, or a combination of these, the quantity of MEK1 protein in the TPL2ΔC co-expressed with MEK1 group was much higher than in the other groups. Phosphorylated ERK (P-ERK) levels were also greater in this group. The red circle indicates the band where MEK1 was expressed alone. GAPDH was the internal control. (B) The quantitative analysis of band intensity from the Western blot pictures in (A) is shown as a fold change compared to the Mock group and normalized to GAPDH. Representative blot from one independent experiment. No statistical analysis was performed due to limited repeats.

4.Disscussion

The goal of this study was to investigate the mechanism by which the TPL2 serine/threonine kinase (also known as MAP3K8), a MAPK signalling pathway kinase that resides in the cytosol, translocated into the nucleus. During these experiments, an interaction was observed between TPL2 and MEK1, and we also observed that TPL2 may affect or facilitate the nuclear localization of MEK1, suggesting that TPL2 has additional roles beyond functioning as an upstream kinase to MEK1 and ERK1/2. Although this study did not directly test TRIM4 involvement, the results align with the model that TRIM4-mediated ubiquitination constrains TPL2 nuclear activity.

The data shows that TPL2 is not only a MAP3K, but also a regulator of MEK1 stability and subcellular localization. This study used fluorescence microscope, immunoprecipitation, and subcellular fractionation experiments to show that TPL2 controls not only the level of MEK1 protein but also its subcellular distribution. The effect of TPL2 on MEK1 levels depended on how active its kinase was, as well as its C-terminus. Overexpression of a C-terminal deletion mutant of TPL2 (TPL2ΔC), which is known to be more stable (Belich et al., 1999) led to an increase in MEK1 protein and some accumulation in the nucleus. A kinase-dead mutant ($TPL2^{D270A}$) did not increase MEK1 levels and showed reduced levels of MEK1 protein under all conditions. To investigate further whether TPL2 could have a direct effect on MEK1 nuclear translocation, we tested a MEK1 mutant lacking the TPT motif (AAA-MEK1), which is required for importin7-mediated nuclear import (Chuderland et al., 2008). Co-expression with TPL2 enhanced nuclear accumulation of AAA-MEK1, suggesting that TPL2 can assist with MEK1 nuclear entry without utilizing importins. These findings provide evidence that TPL2 functions as a MAP3K that regulates MEK1 stability and subcellular localization. Moreover, it appears that these effects are distinct regarding both structure and enzymatic activity, suggesting that TPL2 may regulate MAPK signalling dynamics in some settings through noncanonical pathways that involve interactions with

nuclear signalling intermediates.

4.1 TPL2 exhibits kinase-and NES-dependent subcellular distribution.

Although TPL2 is considered a cytoplasmic MAP3K responsible for transducing TNF and TLR receptor signals to the ERK pathway (Dumitru et al., 2000), previous studies have shown that it contains a functional nuclear export signal (NES) that retains TPL2 in the cytoplasm via a CRM1-dependent mechanism (Collins et al,2019). In this study, I used a GFP-labelled TPL2 construct to analyse the regulatory role of different domains in the subcellular localization of TPL2. The NES deletion mutant (TPL2ΔNES) showed significant GFP signal accumulation in the nucleus and perinuclear region, further validating the crucial role of NES and CRM1-mediated nuclear export in TPL2 localization (Lang et al., 2004).

Conversely, the kinase-inactivating mutant $TPL2^{D270A}$ exhibited a weaker and more diffuse fluorescence signal, with no significant intranuclear accumulation observed. This phenomenon may reflect decreased protein stability or conformational changes in this mutant, and the possibility of restricted nucleoplasm transport mechanisms cannot be ruled out. Notably, one hypothesis is that TPL2 nuclear localization may depend on its kinase activity-mediated binding to specific nuclear proteins; loss of enzymatic activity prevents the formation of these complexes, thus limiting nuclear importation. However, current data are insufficient to support this model.

To further validate this hypothesis, future studies could consider examining the cellular localization patterns of mutants with kinase activity but truncated structures (e.g., C-terminal deletion), or stabilizing the expression levels of wild-type and mutant TPL2 using proteasome inhibitors such as MG132, thereby clarifying the causal relationship between stability and localization.

In summary, our results again validate the crucial role of NES in the cytoplasmic localization of TPL2. However, whether kinase activity further influences its subcellular distribution by regulating protein stability or its binding affinity to

protein complexes remains to be fully understood and may require further investigation using additional experimental approaches and variables. In addition, this study was mainly based on overexpression systems and static imaging analysis, which may not fully reflect endogenous trafficking dynamics under physiological conditions. Furthermore, several experiments were performed , and therefore the reproducibility and biological variability of some observations require further validation. Future studies using endogenous models, biological replicates, live-cell imaging, and additional mechanistic assays may help further clarify the relationship between TPL2 kinase activity, stability, and nuclear-cytoplasmic localization.

4.2 MEK1 stability and localization are regulated by TPL2.

This experiments' results reveal that TPL2 affects MEK1 stability and localization in a variant-specific manner. $TPL2^{WT}$ leads to a modest increase in MEK1 levels, while other TPL2 mutations display more pronounced effects. The C-terminal truncation mutant (TPL2ΔC) is associated with further enhanced MEK1 protein levels, while the kinase-inactive mutation ($TPL2^{D270A}$) confers reduced MEK1 protein levels. It is also possible that the elevated expression level of TPL2ΔC itself contributes to the observed stabilization of MEK1, and this possibility cannot be ruled out. These divergent observations suggest that TPL2 may regulate MEK1 stability through two independent mechanisms: one mechanism dependent on its kinase activity and another mediated by its C-terminal domain. This finding is consistent with previous studies demonstrating that post-translational modifications including phosphorylation as well as scaffold or chaperone proteins that alter the accessibility of E3 ubiquitin ligases regulate MEK1 turnover (Brennan et al., 2011; Dougherty et al., 2005). TPL2ΔC also facilitates ERK activation, which may reflect a potential gain-of-function effect, although further experiments are needed to confirm this.

One possibility is that removal of the PEST domain alters conformational dynamics of TPL2, thereby stabilizing the TPL2-MEK1 complex, potentially protecting

MEK1 from degradation. Although current data cannot distinguish whether TPL2 directly transports MEK1 into the nucleus or indirectly stabilizes it, the observed co-localization pattern supports a piggyback entry model as the most parsimonious explanation. Similar mechanisms have been reported for other MAPK cascade components such as KSR1, which stabilizes MEK1 by forming a scaffold complex and preventing its proteasomal degradation (Roy et al., 2002; Matheny and White, 2006).

Lastly, even though these results are still preliminary, they suggest that TPL2 might function as a bifunctional regulator of MEK1 by influencing both its subcellular compartmentalization and its stability against proteasomal degradation. However, this study has several limitations. Some experiments were performed only once, and the findings were mainly based on overexpression systems and static imaging analysis, which may not fully reflect endogenous cellular dynamics. In addition, the precise mechanism underlying TPL2-MEK1 trafficking remains unclear. Subsequent investigations employing live-cell imaging, biological replicates, or quantitative biophysical assays may help determine whether TPL2-MEK1 interactions form stable complexes with defined stoichiometry and whether MEK1 additionally facilitates the nuclear translocation of TPL2. The unexpected nuclear translocation of AAA-MEK1 in the presence of TPL2 further supports the possibility that TPL2 may utilize MEK1 as a co-transport partner, providing additional insight into the role of TPL2 in subcellular signaling dynamics.

4.3 Structural and catalytic features of TPL2 that regulate MEK1 stability.

This study aimed to determine the impact of certain structural and catalytic properties of TPL2 on its ability to regulate MEK1 stability, as indicated by the effect of TPL2 variants on MEK1 protein levels (Section 4.2). In cytoplasmic co-immunoprecipitation assays, the physical interaction between TPL2 and MEK1 was

not obvious. However, changes in MEK1 protein levels in TPL2 variants suggest that functional coupling extends beyond simple binding affinity.

A C-terminal truncation mutant of TPL2 (TPL2ΔC) that deleted residues 397-467, including a putative PEST degradation motif and part of the ERK-binding domain (Lang et al., 2004), was more effective at raising MEK1 levels than wild-type and kinase-inactive TPL2. This effect may not be solely attributable to differences in TPL2 expression levels, suggesting that the truncated form might possess enhanced functional properties. Consistent with previous studies (Lang et al., 2004), deletion of the PEST domain-containing region stabilized TPL2 protein. This may indirectly increase MEK1 levels by inhibiting its degradation. Our findings support the model that TPL2ΔC acts as a more stable interacting platform that enhances MEK1 stability and protects it from degradation.

On the other hand, $TPL2^{D270A}$ maintained the same form, but was unable to maintain high levels of MEK1. This may mean that MEK1 is being moved to a different part of the cell, but the fact that it is still being depleted suggests how important TPL2 kinase activity is for maintaining MEK1 stability. One possible explanation is that TPL2-mediated phosphorylation modifies the structure of MEK1 or enhances its accessibility to E3 ubiquitin ligases, thereby extending its half-life. Similar protective mechanisms have been found in other MAP3K-MAP2K complexes, where kinase activation alters the likelihood of downstream effector degradation (Dougherty et al., 2005).

In summary, TPL2 affects MEK1 homeostasis through two independent but complementary mechanisms: (1) its kinase activity maintains MEK1 population-dependent phosphorylation, resisting ubiquitination degradation; (2) its C-terminal structure acts as a regulatory element, which may induce the recruitment of degradation factors or control the exposure of MEK1 degradation signals. When both aspects are compromised (e.g., full-length kinase-dead mutants), the decrease in MEK1 levels is more pronounced. On the other hand, enhanced stability is

observed when inhibitory structures (such as TPL2ΔC) are removed. Suggesting a potential auto-inhibitory or degradation-promoting role for this domain.

4.4 Implications for proteasomal regulation and post-translational control

This section further investigates the underlying mechanism, focusing on post-translational regulation. This is based on the differential effects of the different TPL2 variants on MEK1 protein levels described above. Although transcriptional effects cannot be completely ruled out, the rapid and variant-specific changes in MEK1 abundance suggest that it is primarily determined by protein homeostasis mechanisms.

Our findings raise the possibility that TPL2 contributes to MEK1 stabilization by limiting its ubiquitin-mediated proteasomal degradation, although this mechanism was not directly tested in the current study. Previous studies have shown that the phosphorylation status of MEK1, as well as its interaction with stabilizing partners such as scaffold proteins, affect its stability (Brennan et al., 2011; Dougherty et al., 2005). In this context, TPL2 may act both as an upstream kinase for MEK1 and as a scaffold to protect it from the degradation machinery. In TPL2ΔC, the conventional C-terminal PEST motif (a degradation signal associated with rapid degradation) (Rechsteiner and Rogers, 1996) is missing, thus, it may be more stable and provide enhanced protection of MEK1 through persistent binding or spatial sequestration.

Although this study did not directly find evidence of MEK1 ubiquitination, the findings support a hypothesis that TPL2 affects the MEK1 half-life through post-translational regulation. MEK1 degradation kinetics experiments with various TPL2 variants are needed to validate future studies. In addition, MEK1 ubiquitination can be assessed under different TPL2 expression conditions using

ubiquitin pull-down and immunoblotting assays. Stability assays using proteasome inhibitors such as MG132 can further determine whether MEK1 degradation is proteasome-dependent or regulated by TPL2.

Notably, the subcellular environment of MEK1 degradation may be critical. When the catalytic activity of TPL2 is impaired or its localization is altered, MEK1 may accumulate abnormally in the nucleus. In this region, MEK1 may be more susceptible to proteasomal degradation, possibly due to reduced interaction with stabilizing scaffold proteins or increased activity of nuclear-localized ubiquitin ligases. This may occur because TPL2 and MEK1 create a complex with TPL2 as a scaffolding protein, which means that they don't need typical nuclear localization signals. This phenomenon is consistent with the review by Cargnello et al. (2011), who pointed out that the subcellular localization of MAPK signalling is finely regulated by the assembly of scaffold proteins and kinase complexes, which may indirectly affect the distribution of key kinases such as MEK1. At the same time, Ben-Addi et al. (2014) found that this complex is necessary for the activation of ERK1/2 signalling by studying the formation mechanism of the TPL2-14-3-3 complex, suggesting that TPL2 regulates the spatial organization of the MAPK signalling cascade through protein interaction, although its direct involvement in the nuclear transposition of MEK1 remains to be further demonstrated.

Further research is required to determine whether MEK1 stability is directly regulated by TPL2-dependent phosphorylation or by subcellular environment-specific degradation pathways. Other MAPK components are also subject to regulated nuclear inactivation and feedback control mechanisms (Janes et al., 2008). This further supports the idea that subcellular compartmentalization is closely linked to proteasomal regulation.

In summary, TPL2 can regulate MEK1 steady-state expression levels through two mechanisms: firstly, the structural integrity of TPL2, particularly its C-terminal region, can enhance MEK1 stability independently of kinase activity by disrupting

the exposure of MEK1 ubiquitin tags, interfering with protein-protein interactions, or limiting its recruitment to degradation complexes; secondly, TPL2's kinase activity itself plays a crucial regulatory role, potentially inhibiting the ubiquitination and proteasome-mediated degradation of MEK1 by phosphorylating MEK1 or its degradation regulators. Both mechanisms appear to be indispensable during the upregulation of MEK1, suggesting that TPL2 functions not only as an upstream kinase in MAPK signalling but also as a scaffolding protein that stabilizes crucial signalling components. Although the scaffolding function of TPL2 was not examined in this study, it is consistent with the findings of Fahey et al. (2025), who showed that TPL2 acts as both a kinase and a scaffolding protein to maintain ABIN2 and p105. This complex regulatory mechanism likely operates primarily within the cytoplasmic or perinuclear MAPK signalling microenvironment and plays a crucial role in maintaining the activity levels of the MEK1 protein.

Taken together, these findings suggest that TPL2 has a functional range beyond its traditional kinase role. TPL2 acts as a dual catalytic and stabilizing factor to dynamically regulate MEK1 protein turnover in response to changes in localization, domain accessibility and proteolytic signals. TPL2's dual function makes it an integration node between MAPK activation and degradation, so its post-translational regulation in the signalling pathway needs to be further studied.

4.5 Future directions and therapeutic relevance

Although this study establishes a role for TPL2 in regulating MEK1 stability and localization, several mechanistic and translational questions remain. Most critically, it is currently unclear whether TPL2 directly interferes with MEK1 ubiquitination or indirectly through altering subcellular trafficking or interactions with auxiliary stabilizing proteins. An important direction for future studies is to distinguish between these possibilities using targeted biochemical approaches. For example, the ubiquitination pattern of MEK1 under different TPL2 variants can be revealed by blotting the immunoprecipitated MEK1 with ubiquitin-specific antibodies. Real-

time degradation experiments combined with protein synthesis inhibitors (such as cycloheximide) and proteasome inhibitors (such as MG132) can clarify whether TPL2 mainly affects the degradation or synthesis of MEK1. Further proximity labelling or cross-linking-based interactomes techniques may also discover new TPL2-dependent MEK1 stabilizing factors.

Beyond the mechanistic exploration, this study also raises an important therapeutic question: can the scaffold function of MAP3K kinases be exploited for disease intervention? MEK1 and ERK are the core signalling molecules of many tumors (such as melanoma, colorectal cancer, and pancreatic cancer). MEK inhibitors (such as trametinib and cobimetinib) have been used in clinical practice, but the efficacy is often not long-lasting due to feedback loops and pathway reactivation (Caunt et al., 2015). Given that TPL2 can regulate the abundance and localization of MEK1 without necessarily triggering complete MAPK activation, it may become a potential therapeutic target, especially by interfering with its non-enzymatic scaffold functional region. Such strategies could either sensitize cancer cells to conventional inhibitors by stabilizing or redistributing MEK1 or reduce the proliferative and survival capacity of tumour cells by reducing its availability in the nucleus.

Finally, this study highlights a broader principle in kinase biology: upstream kinases often have dual roles, not only catalysing phosphorylation but also shaping the spatiotemporal dynamics of their substrates. The identification of TPL2 as a spatial regulator of MEK1 provides direction for further exploration of other members of the MAPK cascade. These members may also have the phenomenon of separation of catalytic domain and domain function. In the future, targeting these dual-function regions may provide new signal reprogramming methods for diseases related to excessive activation of pathological pathways, and may achieve a better balance between specificity and toxicity.

4.6 Challenges and limitations

This study has several limitations that should be considered when interpreting the findings. First, due to time limitations and the exploratory nature of this project, most experiments were only performed once and did not include sufficient biological or technical repeats. As a result, although grayscale quantification was performed using ImageJ, statistical analysis and error bar presentation could not be included. Therefore, the current findings should be interpreted as preliminary observations rather than definitive conclusions. Nevertheless, the overall trends observed across multiple experimental approaches remained generally consistent and provided useful direction for subsequent experiments.

Another important limitation relates to imaging quality and spatial resolution. Some fluorescence imaging experiments were conducted using relatively low magnification microscopy, which limited the ability to accurately assess detailed nuclear and cytoplasmic localization patterns. Although clear localization differences could still be observed between different TPL2 mutants, higher magnification confocal imaging and live-cell imaging approaches would provide more precise analysis of protein trafficking dynamics and localization behavior.

This study also relied heavily on transient overexpression systems in HEK293T and COS-7 cells. While these cell lines are commonly used because of their high transfection efficiency and suitability for mechanistic studies, overexpression itself may artificially alter protein stability, localization, or interaction dynamics. Therefore, the observed TPL2-MEK1 interactions may not fully reflect endogenous physiological conditions. Future studies using endogenous tagging approaches or stable cell systems would help address this limitation.

Although the data suggest that TPL2 may regulate MEK1 stability through post-translational mechanisms, the current study did not directly examine ubiquitination or proteasomal degradation pathways. No ubiquitination assays were performed to determine whether TPL2 affects MEK1 ubiquitination status. In addition,

proteasome inhibition experiments using inhibitors such as MG132 were not carried out. Therefore, the proposed relationship between TPL2 structure and MEK1 degradation remains speculative and requires further validation.

Despite these limitations, this study provides preliminary evidence suggesting that TPL2 may regulate both the stability and subcellular localization of MEK1 through mechanisms involving kinase activity and structural domains. These findings establish a foundation for future mechanistic studies investigating the non-canonical functions of TPL2 in MAPK signaling regulation.

Reference

Adachi, M., Fukuda, M., & Nishida, E. (1999). Two co-existing mechanisms for nuclear import of MAP kinase: passive diffusion of a monomer and active transport of a dimer. *The EMBO journal*, *18*(19), 5347–5358. https://doi.org/10.1093/emboj/18.19.5347

Barbacid, M. (1987). *ras genes*. *Annual Review of Biochemistry*, 56(1), 779–827. https://doi.org/10.1146/annurev.bi.56.070187.004023

Bansod, S., Dodhiawala, P. B., Geng, Y., Bulle, A., Liu, P., Li, L., Lim, K. H. (2024). The TRIM4 E3 ubiquitin ligase degrades TPL2 and is modulated by oncogenic KRAS. Cell Reports, 43(6), 113279. 10.1016/j.celrep.2024.114667

Beinke, S., & Ley, S. C. (2004). *Functions of NF-κB1 and NF-κB2 in immune cell biology*. *Biochemical Journal*, 382(2), 393–409. https://doi.org/10.1042/BJ20040544

Beinke, S., Robinson, M. J., Hugunin, M., & Ley, S. C. (2004). Lipopolysaccharide Activation of the TPL-2/MEK/Extracellular Signal-Regulated Kinase Mitogen-Activated Protein Kinase Cascade Is Regulated by IκB Kinase-Induced Proteolysis of NF-κB1 p105. *Molecular and Cellular Biology*, *24*(21), 9658–9667. https://doi.org/10.1128/MCB.24.21.9658-9667.2004

Belich, M. P., Salmeron, A., Johnston, L. H., & Ley, S. C. (1999). *TPL-2 kinase regulates the proteolysis of the NF-κB-inhibitory protein NF-κB1 p105*. *EMBO Journal*, 18(24), 6882–6893. https://doi.org/10.1093/emboj/18.24.6882

Ben-Addi, A., Mambole-Dema, A., & Brender, C. (2014). *IκB kinase–induced interaction of TPL-2 kinase with 14-3-3 is essential for Toll-like receptor activation of ERK-1 and -2 MAP kinases. Proceedings of the National Academy of Sciences*, 111(14), E1428–E1437. https://doi.org/10.1073/pnas.1320440111

Brennan, D. F., Dar, A. C., Hertz, N. T., Chao, W. C., Burlingame, A. L., Shokat, K. M., & Barford, D. (2011). *A Raf-induced allosteric transition of KSR stimulates phosphorylation of MEK*. *Nature*, 472(7343), 366–369. https://doi.org/10.1038/nature09860

Breyer, F. (2020). *Regulation of phagosome maturation and bacterial killing by the TPL-2 complex* [Doctoral dissertation, University College London]. *UCL Discovery*. https://discovery.ucl.ac.uk/id/eprint/10117819/

Cargnello, M., & Roux, P. P. (2011). Activation and function of the MAPKs and their substrates, the MAPK-activated protein kinases. *Microbiology and molecular biology reviews: MMBR*, *75*(1), 50–83. https://doi.org/10.1128/MMBR.00031-10

Caunt, C. J., Sale, M. J., Smith, P. D., & Cook, S. J. (2015). MEK1 and MEK2 inhibitors and cancer therapy: the long and winding road. Nature Reviews Cancer, 15(10), 577–592. https://doi.org/10.1038/nrc4000

Choi, S. Y., Kim, D. S., Park, S. H., Lee, K. S., Seo, Y. J., Park, J. Y., & Lee, J. H. (2008). UVB-induced MAPK activation and histone H3 phosphorylation require Tpl2 kinase. Journal of Investigative Dermatology, 128(2), 405–415. https://doi.org/10.1038/sj.jid.5701032

Chuderland, D., Konson, A., & Seger, R. (2008). Identification and characterization of a general nuclear translocation signal in signaling proteins. Molecular Cell, 31(6), 850–861. https://doi.org/10.1016/j.molcel.2008.08.007

Collins, P. E., Somma, D., Kerrigan, D., Herrington, F., Keeshan, K., Nibbs, R. J. B., & Carmody, R. J. (2019). The IκB-protein BCL-3 controls Toll-like receptor-induced MAPK activity by promoting TPL-2 degradation in the nucleus. *Proceedings of the National Academy of Sciences of the United States of America*, *116*(51), 25828–25838. https://doi.org/10.1073/pnas.1900408116

Dougherty, M. K., Müller, J., Ritt, D. A., Zhou, M., Zhou, X. Z., Lu, K. P., & Morrison, D. K. (2005). Regulation of Raf-1 by direct feedback phosphorylation. Molecular Cell, 31(6), 830–841. https://doi.org/10.1016/j.molcel.2004.11.055

Dumitru, C. D., Ceci, J. D., Tsatsanis, C., Kontoyiannis, D., Stamatakis, K., Lin, J. H., Patriotis, C., Jenkins, N. A., Copeland, N. G., Kollias, G., & Tsichlis, P. N. (2000). TNF-α induction by LPS is regulated posttranscriptionally via a Tpl2/ERK-dependent pathway. Nature Immunology, 1(6), 545–551. https://doi.org/10.1016/S0092-8674(00)00210-5

Ebert, P. J. R., Cheung, J., Yang, Y., McNamara, E., Hong, R., Moskalenko, M., Gould, S. E., Maecker, H., Irving, B. A., Kim, J. M., Belvin, M., & Mellman, I. (2016). MAPK pathway inhibition sensitizes tumor cells to T cell-mediated cytotoxicity. Cancer Research, 76(1), 114–126. https://doi.org/10.1016/j.immuni.2016.01.024

Fahey, D. L., Patel, N., & Watford, W. T. (2025). TPL2 kinase activity is required for Il1b transcription during LPS priming but dispensable for NLRP3 inflammasome activation. Frontiers in immunology, 16, 1496613. https://doi.org/10.3389/fimmu.2025.1496613

Flaherty, K. T., Puzanov, I., Kim, K. B., Ribas, A., McArthur, G. A., Sosman, J. A., O'Dwyer, P. J., Lee, R. J., Grippo, J. F., Nolop, K., & Chapman, P. B. (2010).

Inhibition of mutated, activated BRAF in metastatic melanoma. New England Journal of Medicine, 363(9), 809–819. https://doi.org/10.1056/NEJMoa1002011

Gantke, T., Sriskantharajah, S. & Ley, S. (2011) Regulation and function of TPL-2, an IκB kinase-regulated MAP kinase kinase kinase. *Cell Res* 21, 131–145 https://doi.org/10.1038/cr.2010.173

González, F. A., Raden, D. L., & Davis, R. J. (1993). Identification of substrate recognition determinants for human ERK1 and ERK2 protein kinases. Journal of Biological Chemistry, 268(24), 18427–18433 https://doi.org/10.1016/S0021-9258(18)54548-8

Hao, J., Cao, Y., Yu, H., Zong, L., An, R., & Xue, Y. (2021). Effect of MAP3K8 on prognosis and tumor-related inflammation in renal clear cell carcinoma. Frontiers in Genetics, 12, 674613. https://www.frontiersin.org/articles/10.3389/fgene.2021.674613/full

Holderfield, M., Deuker, M. M., McCormick, F., & McMahon, M. (2014). Targeting RAF kinases for cancer therapy: BRAF-mutated melanoma and beyond. *Nature Reviews Cancer, 14(7),* 455–467. https://doi.org/10.1038/nrc3760

Hou, P., & Wang, Y. A. (2022). Conquering oncogenic KRAS and its bypass mechanisms. Theranostics, 12(13), 5691–5709. https://doi.org/10.7150/thno.71260

Ip, Y. T., & Davis, R. J. (1998). Signal transduction by the c-Jun N-terminal kinase (JNK)from inflammation to development. Current Opinion in Cell Biology, 10(2), 205–219. https://doi.org/10.1016/s0955-0674(98)80143-9

Janes, K. A., Reinhardt, H. C., & Yaffe, M. B. (2008). Cytokine-induced signaling networks prioritize dynamic range over signal strength. *Cell*, 135(2), 343–354. https://doi.org/10.1016/j.cell.2008.08.051

Khokhlatchev, A. V., Canagarajah, B., Wilsbacher, J., Robinson, M., Atkinson, M., Goldsmith, E. J., & Cobb, M. H. (1998). Phosphorylation of the MAP kinase ERK2 promotes its dissociation from MEK1 and nuclear translocation. Cell, 93(5), 605–615. 10.1016/S0092-8674(00)81189-7

Kudo, N., Wolff, B., Sekimoto, T., Schreiner, E. P., Yoneda, Y., Yanagida, M., Horinouchi, S., & Yoshida, M**.** (1998). Leptomycin B inhibition of signal-mediated nuclear export by direct binding to CRM1. *Experimental Cell Research, 242*(2), 540–547. https://doi.org/10.1006/excr.1998.4136

Lake, D., Corrêa, S. A. L., & Müller, J. (2016). Negative feedback regulation of the ERK1/2 MAPK pathway. Cellular and Molecular Life Sciences, 73(23), 4397–4413. https://doi.org/10.1007/s00018-016-2297-8

Lang, V., Symons, A., Watton, S. J., Janzen, J., Soneji, Y., Beinke, S., Howell, S., & Ley, S. C. (2004). ABIN-2 forms a ternary complex with TPL-2 and NF-kappa

B1 p105 and is essential for TPL-2 protein stability. *Molecular and cellular biology*, *24*(12), 5235–5248. https://doi.org/10.1128/MCB.24.12.5235-5248.2004

Lailler, C., Louandre, C., Morisse, M. C., et al. (2019). ERK1/2 signaling regulates the immune microenvironment and macrophage recruitment in glioblastoma. *Bioscience Reports, 39(9).* https://doi.org/10.1042/BSR20191433

Lee, J., Rhee, M. H., Kim, E., & Cho, J. Y. (2015). Tumor progression locus 2 (Tpl2) kinase as a novel therapeutic target for cancer: double-sided effects of Tpl2 on cancer. *International Journal of Molecular Sciences*, 16(3), 4471–4491. https://doi.org/10.3390/ijms16034471

Lito, P., Rosen, N., & Solit, D. B. (2013). Tumor adaptation and resistance to RAF inhibitors. *Nature Medicine, 19(11),* 1401–1409. https://doi.org/10.1038/nm.3392Martin-Vega, A., & Cobb, M. H. (2023).

Matheny, S. A., & White, M. A. (2006). Ras regulates assembly of mitogenic signalling complexes through the effector protein IMP. Nature, 439, 228–232. 10.1038/nature02237

McCubrey J. Andrew, Steelman L. S., Chappell W. H., Abrams S. L., Franklin R. A., Montalto G., Cervello M., Libra M., Candido S., Malaponte G., Mazzarino M. C., Fagone P., Nicoletti F., et al (2012). Ras/Raf/MEK/ERK and PI3K/PTEN/Akt/mTOR Cascade Inhibitors: How Mutations Can Result in Therapy Resistance and How to Overcome Resistance. Oncotarget; 3: 1068-1111. https://www.oncotarget.com/article/659/text/

Moon, H., & Ro, S. W. (2021). MAPK/ERK Signaling Pathway in Hepatocellular Carcinoma. *Cancers*, *13*(12), 3026. https://doi.org/10.3390/cancers13123026

Njunge, L. W., Estania, A. P., Guo, Y., Liu, W., & Yang, L. (2020). Tumor progression locus 2 (TPL2) in tumor-promoting Inflammation, Tumorigenesis and Tumor Immunity. Theranostics, 10(18), 8343–8364. https://doi.org/10.7150/thno.45848

Patel, M., Eckburg, A., Gantiwala, S., Hart, Z., Dein, J., Lam, K., & Puri, N. (2021). Resistance to Molecularly Targeted Therapies in Melanoma. *Cancers*, *13*(5), 1115. https://doi.org/10.3390/cancers13051115

Plotnikov, A., Zehorai, E., Procaccia, S., & Seger, R. (2011). The MAPK cascades: Signaling components, nuclear roles and mechanisms of nuclear translocation. Biochimica et Biophysica Acta (BBA) - Molecular Cell Research, 1813(9), 1619–1633. https://doi.org/10.1016/j.bbamcr.2010.12.012

Rechsteiner, M., & Rogers, S. W. (1996). PEST sequences and regulation by proteolysis. Trends in Biochemical Sciences, 21(7), 267–271.

Reiser, V., Ammerer, G., & Ruis, H. (1999). Nucleocytoplasmic traffic of MAP kinases. *Gene expression*, *7*(4-6), 247–254. https://doi.org/10.1016/S0968-0004(96)10031-1

Ritt, D. A., Monson, D. M., Specht, S. I., & Morrison, D. K. (2010). Impact of feedback phosphorylation and Raf heterodimerization on normal and mutant B-Raf signaling. *Molecular and cellular biology*, *30*(3), 806–819. https://doi.org/10.1128/MCB.00569-09

Roy, F., Laberge, G., Douziech, M., Ferland-McCollough, D., & Therrien, M. (2002). KSR is a scaffold required for activation of the ERK/MAPK module. Genes & Development, 16(4), 427–438. 10.1101/gad.962902

Robinson, M. J., Beinke, S., Kouroumalis, A., Tsichlis, P. N., & Ley, S. C. (2007). Phosphorylation of TPL-2 on Serine 400 Is Essential for Lipopolysaccharide Activation of Extracellular Signal-Regulated Kinase in Macrophages. *Molecular and Cellular Biology*, *27*(21), 7355–7364. https://doi.org/10.1128/MCB.00301-07

Samatar, A., Poulikakos, P. (2014). Targeting RAS–ERK signalling in cancer promises and challenges. *Nat Rev Drug Discov* 13, 928–942.https://doi.org/10.1038/nrd4281

Sebolt-Leopold, J. S., & Herrera, R. (2004). Targeting the mitogen-activated protein kinase cascade to treat cancer. *Nature reviews. Cancer*, *4*(12), 937–947. https://doi.org/10.1038/nrc1503

Sundaram, M. V. (2006). RTK/Ras/MAPK signaling. WormBook, 1–19. https://doi.org/10.1895/wormbook.1.80.1

Varshavsky, A. (2011). The N-end rule pathway and regulation by proteolysis. *Protein Science, 20*(8), 1298–1345. https://doi.org/10.1002/pro.666

Wee, S., Jagani, Z., Xiang, K. X., Loo, A., Dorsch, M., Yao, Y. M., Sellers, W. R., Lengauer, C., & Stegmeier, F. (2009). PI3K pathway activation mediates resistance to MEK inhibitors in KRAS mutant cancers. *Cancer research*, *69*(10), 4286–4293. https://doi.org/10.1158/0008-5472.CAN-08-4765

Wang, G., Wang, J., Chang, A. et al. Her2 promotes early dissemination of breast cancer by suppressing the p38 pathway through Skp2-mediated proteasomal degradation of Tpl2. Oncogene 39, 7034–7050 (2020). https://doi.org/10.1038/s41388-020-01481-y

Xia, L., Zhang, D., Du, R., Wang, L., Hu, W., & Xu, L. (2021). OVOL2 attenuates the expression of MAP3K8 to suppress epithelial mesenchymal transition in colorectal cancer. *Pathology - Research and Practice, 223*, 153476, https://doi.org/10.1016/j.prp.2021.153493

Xu, D., Matsumoto, M. L., McKenzie, B. S., & Zarrin, A. A. (2018). TPL2 kinase action and control of inflammation. *Pharmacological research*, *129*, 188–193. https://doi.org/10.1016/j.phrs.2017.11.031

You, Y., Wen, D., Zeng, L., Lu, J., Xiao, X., Chen, Y., Song, H., & Liu, Z. (2022). ALKBH5/MAP3K8 axis regulates PD-L1+ macrophage infiltration and promotes hepatocellular carcinoma progression. *International journal of biological sciences*, *18*(13), 5001–5018. https://doi.org/10.7150/ijbs.70149

Zhang, D., Huang, J., Wang, F. et al. BMI1 regulates multiple myeloma-associated macrophage's pro-myeloma functions. Cell Death Dis 12, 495 (2021). https://doi.org/10.1038/s41419-021-03748-y